



**Politecnico
di Torino**



**Politecnico di Torino
Technische Universität Wien**

Master of Science in Environmental and Land Engineering
Natural Risk and Civil Protection

**The effect of multiple reservoirs on flood peak
reduction: the case of two austrian catchments**

Supervisor: Prof. Alberto Viglione

Co-supervisors: Prof. Gunter Blöschl

Proj. Ass. Miriam Bertola

Student: Anna Basso

March 2024

Summary

Abstract	v
1 Introduction	1
2 Data availability and study area	8
2.1 Data availability	8
2.1.1 Data on catchments and river network	8
2.1.2 Flooding data	8
2.1.3 Data on dams	10
2.2 Study area	10
3 Methodology for flood peak reduction evaluation	14
3.1 Selection of the computation nodes	15
3.2 Representative dam definition	16
3.3 Effective volume available for flood control	17
3.4 Regionalization of the time constant	18
3.5 Design hydrograph creation	21
3.6 Protection ratio calculation	23
3.7 Filling discharge definition	25
3.8 Application of the peak reduction routine	26

4	Flood peak reduction for design event and comparison to observation	28
4.1	Information at each calculation nodes	28
4.2	Result discussion	35
4.3	Comparison with literature	40
4.4	Results validation	42
4.4.1	GEV distribution	43
4.4.2	Validation in time	46
4.4.3	Validation in space	47
4.4.4	Validation outcomes	49
4.5	Sensitivity analysis	51
4.5.1	Inlet hydrograph changes	52
4.5.2	Filling discharge changes	53
4.5.3	Protection ratio changes	54
5	Conclusions	56
	Acknowledgements	59
	Bibliography	60
	Annexes	65

Abstract

In Austria there are 78 large reservoirs and, in most cases, they are located in nested catchments. The presence of a reservoir generally produces an attenuation effect on flood peaks downstream, however the effect of multiple reservoirs in a catchment remains unclear.

The aim of this work is to analyze the combined effect of multiple dams on flood peaks along the river network at the regional scale. Its evolution is studied in space, considering how the effect changes along the river segments and as a function of the return period of the flood event.

The method used consists in two steps: (i) the design hydrographs are evaluated at several locations along the river network for 30, 100 and 300 years return periods, based on interpolated flood quantiles in ungauged catchments; (ii) the peak reduction is estimated based on the information on dams in the catchment (i.e. number, position, storage capacity and drainage area) and using the concept of *equivalent reservoir*, *protection ratio* and *filling discharge*.

The reservoirs effect is here evaluated as the percentage of reduction of the flood wave peak in river sections downstream of one or several dams. This approach is applied to the *Salzach* and the austrian part of the *Drau catchments*, where there are a fairly large number of dams placed both in series and in parallel with each other.

The results obtained show that the relative peak reduction is greatest at the reservoirs and

decreases rapidly downstream for each of the return periods analyzed and for the different combinations of dams.

The method is validated in both time and space, using data from a number of gauging stations available in these two catchments. Overall the method is able to estimate accurately flood peak attenuation of reservoirs even though the values are generally lower than the observed one, the latter being however based on short samples compared to the return periods of design events.

On the whole the method can be considered a valuable instrument for estimating reservoir induced flood peak reduction in ungauged basins, over the river network at the regional scale.

Chapter 1

Introduction

Rivers, and water resources in general, have always been used by humans for a wide variety of purposes: economic, social and political. Particularly evident in Austria is the use of rivers, given the favorable geography and topography of the country, for hydropower generation: in fact starting from 1898, 78 large dams have been built in Austria (Figure 1.1).

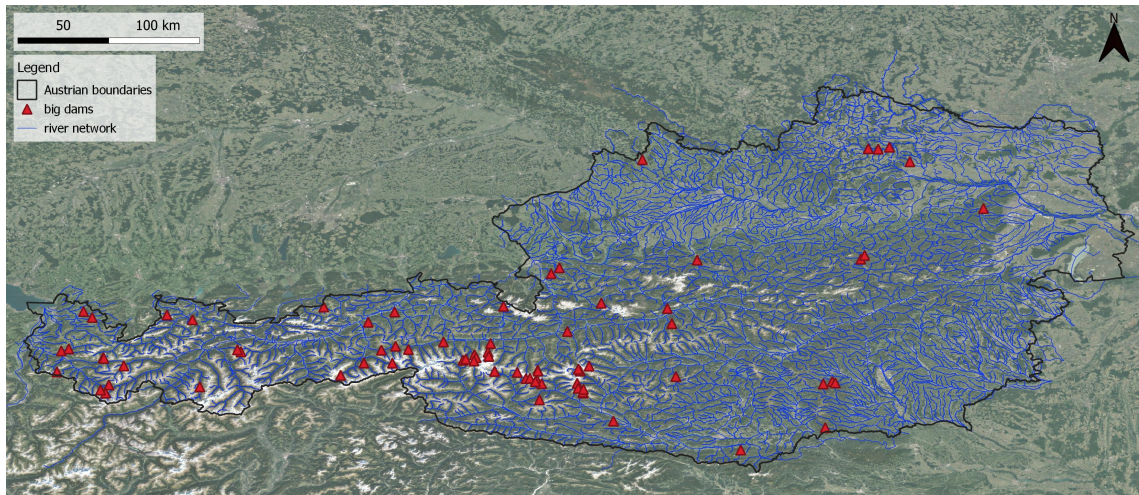


Figure 1.1: Big dams in Austria

Large dams are defined as structures with a height of 15 metres or more, measured from the lowest point of contact to the top of the dam, or with a height between 5 and 15 metres

and having a storage volume bigger than 3 million of cubic metres.

Specifically in the country we have structure with a storage volume varying from a minimum of 30000 cubic meters for the *Subersach Dam*, to a maximum of about 200 millions of cubic meters for the *Kölnbrein Dam*.

These facilities, in addition to allowing energy production, have a complex network of downstream impacts, affecting both physical and biochemical parameters and of course hydrology and the runoff conditions.

As in the study by Muhar et al. (2000), overall 79% of the total number of stream kilometer of austrian largest river are moderated to heavily altered by human activity. The hydrological alteration reaches the 49% of them and this is caused by impoundment (16 %), water diversion (19 %) and hydropeaking (14 %).

In both Merx et Al (2012), Hall et Al (2014) and Bertola et Al (2019) is identified, among the others, as one of the potential drivers of change of the flood regime the river channel engineering and thus the presence of hydraulic structures (Figure 1.2). All of these drivers affect not only the peak, reducing the value of the discharge, but also the timing and shape of the flood hydrographs.

Even though large dams are almost 90% used only for power generation purposes (Annexes: Table 1), they also have the ability to attenuate flood peaks. The effect can be understood from the *S-shape* of the *flood frequency curve* (Figure 1.2): structures reduce the discharge starting from an initial value linked to the dam's rules of use and continue to reduce until the flow rate reaches a value whereby the structure is no longer able to store water and so, be effective.

Peak reduction is related to two factors: to the actual volume of water retained by the structure depending on the availability at the time of the event and to the separation be-

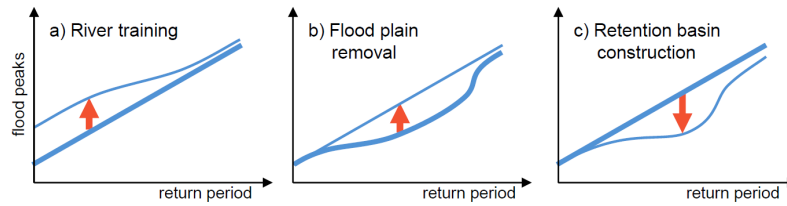


Figure 1.2: Hypothesised impact of three types of hydraulic engineering activities on the *flood frequency curve* (Hall et Al)

tween the flood peaks recorded in the catchments upstream and downstream of the dam due to the lag produced by the structure itself.

Previous studies related to the topic of the effect of dams on floods can be found in the literature.

These include, for example, the studies by Volpi et Al (2018) and Cipollini et Al (2022) whose main goal was to provide a physically based mathematical framework to account for the effect of one or more reservoirs located in series, on the peak flood quantile at the catchment scale. In these studies, reference is made to two indices that summarize in a simple way the factors governing the reduction of the flood wave peak.

Manfreda et Al (2021) developed a mathematical framework to interpret the effect of detention dams on floods, in order to both dimension these structures and investigate flood risk conditions. In this work a simplified form to interpret the outflow of a reservoir was retrieved in order to taking into account not only the inflow but also additional factors that have an huge effect on the flow downstream the structure.

Some studies conducted in Austria analyze the effects of reservoirs on flood peaks by focusing on single notable events or alternatively by analyzing the impact of reservoirs on flood events using long-term runoff or discharge data series, including additional information on diversions and reservoir use rules.

Stecher and Herrnegger (2022) completed a study in which the impact of hydropower reser-

voirs is assessed for different heavily modified catchments in Austria. They calculated the natural unaffected annual peak discharges downstream of the reservoirs by transposing the peak runoff of an unaffected reference catchment by considering the spatial proximity, the catchment area, the land cover and the precipitation conditions in both catchments. The potential impact has been then calculated by comparing the estimated and the observed discharge peaks, coming from the annual maximum floods of the period 1976-2017. The potential *flood peak reduction (FPR)* according to this work can be calculated for every day per year and each location: especially to do the latter they propagated the estimated peak discharge of the directly affected gauge onto these downstream gauges by linearly interpolating the median values along the river stretch.

In general, it is understood from these studies that the reduction is a function of the characteristics of the structure, the rules of its use, its location in the catchment area, thus the portion of the territory controlled by the reservoir, and the season in which the event occurs.

Everything reported so far clarifies how the multiple studies carried out differ from the goal set by this thesis. In fact, they have either focused on smaller scales of analysis than the regional one, or they have focused only on one dam or on one specific combinations of dams or finally they didn't make use of a peak reduction model but analyze changes in data series.

It is common knowledge that the presence of multiple reservoirs in a catchment generally induces the attenuation of flood events, thus mitigating their impact in downstream flood-prone areas.

Here, with this work, we want to understand, in more specific terms, how: dams (i) whose main purpose is not flood control, (ii) that are located significantly upstream, and (iii)

that are complexly combined act on flood waves characterized by different return periods. To evaluate this effect, an approach involving two main steps was applied. The first consists of evaluating the design flood waves at different points in the river network. In the next step, peak reduction is estimated using a method that takes into account the available volume in the dams and their location in the catchment area. The effect of the reservoirs is then evaluated, for each point where the hydrographs were created, as the percentage of peak flood wave reduction.

To check the reliability of this procedure, a validation was performed. Specifically, a number of points were identified where the reduction obtained from the observations available at the measuring stations was compared with that obtained from our model.

Finally, an attempt was made to understand how the model could be improved by performing a sensitivity analysis.

Notice that the method is based on some initial assumptions: first precipitation is considered as uniform over the entire catchment under analysis, an unrealistic assumption for such a large area, and in addition floods climate changing recorded over time both in magnitude (Figure 1.3 and Figure 1.4) and in timing (Figure 1.5) as shown by previous studies by Hall et al (2014) and Blöschl et Al (2017 and 2019) are not included.

These assumptions regarding hydrological and climatic conditions make this method a model that simplifies reality in order to be easier to manage and apply.

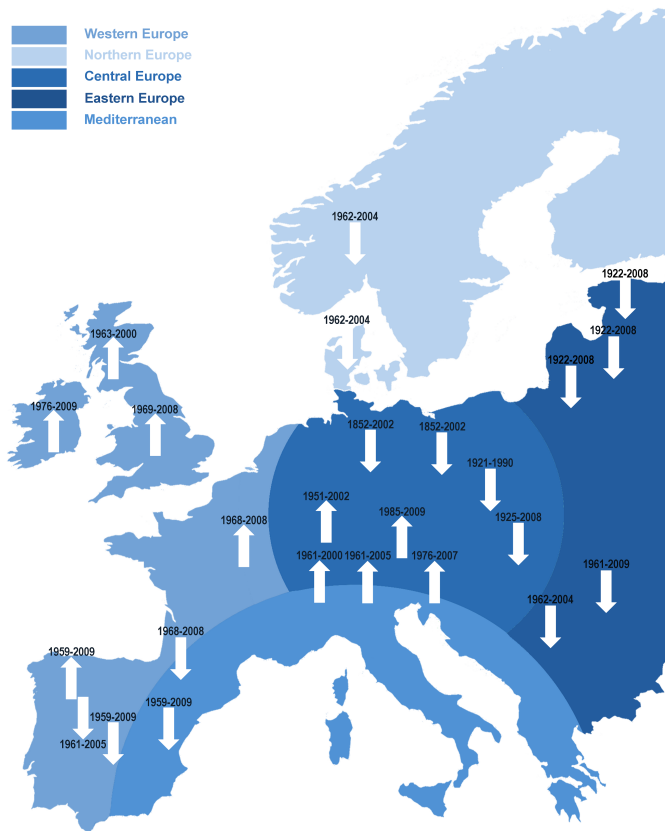


Figure 1.3: Schematic summarising the observed flood changes in Europe (Hall et al)

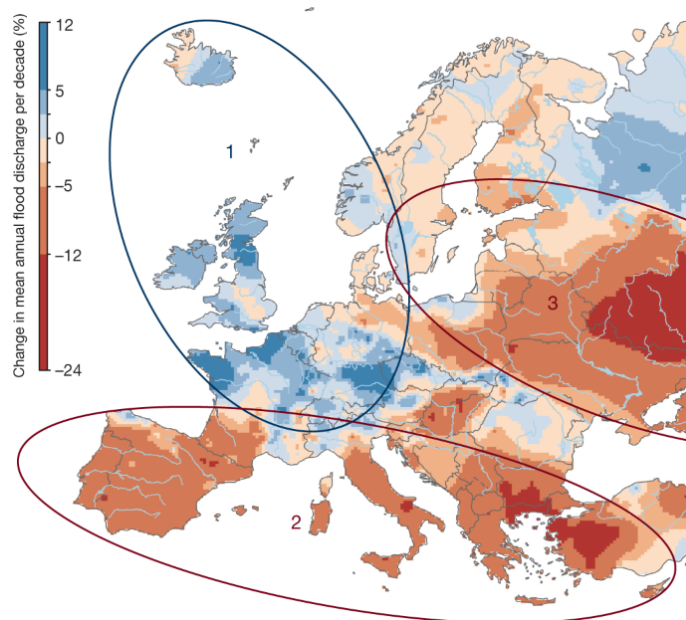


Figure 1.4: Observed regional trends of river flood discharges, 1960–2010 (Blöschl et al)

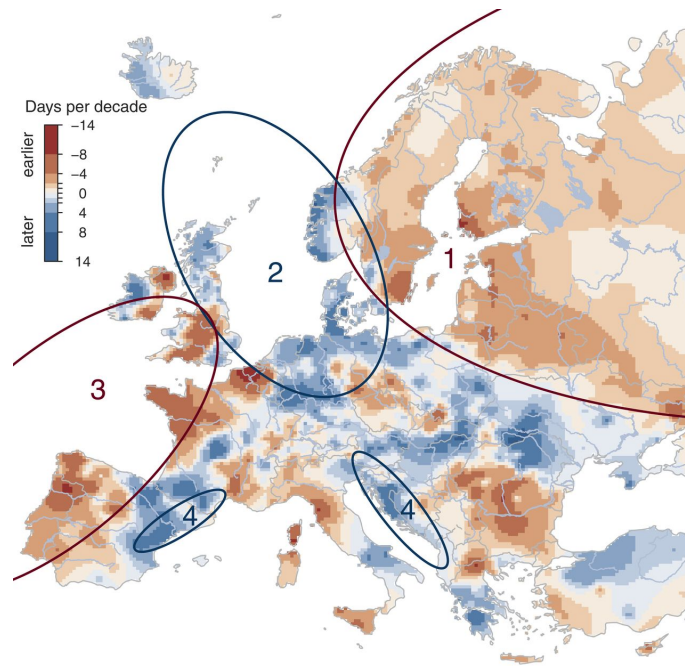


Figure 1.5: Observed trends of river flood timing, 1960–2010 (Blöschl et Al)

Chapter 2

Data availability and study area

2.1 Data availability

2.1.1 Data on catchments and river network

Information on catchments and associated river networks was obtained from the *pan-European database Catchment Characterisation and Modelling (CCM)*.

This dataset includes, in the form of vector files, a hierarchical set of river segments and catchments that allow analysis at various scales. Thanks to this, data on waterbasins area and river stretches length, among other additional information, are available.

2.1.2 Flooding data

In the context of the *HORA 3.0 project (HOchwasserRisikozonierung Austria 3.0)*, through to the collaboration of the *Institute of Hydraulic Engineering and Water Resources Management* of the *TU Wien* and the austrian *local water authorities* the estimation of flood quantiles in ungauged catchments was carried out.

This work evaluates the T-year floods in 21730 ungauged catchments using the first three statistical moments (i.e. mean annual flood, coefficient of variation of maximum annual

floods and coefficient of skewness of maximum annual floods) available for the 782 gauged catchments across Austria. These flood quantiles given above derived from a three steps process: (i) estimation of flood moments at gauged catchments from a series of annual maximum flows, (ii) regionalization of these values using the *topological kriging* and then (iii) final correction of the flood quantiles to take into account the catchments attributes that are strongly correlated to the regionalization process (i.e. catchment area, presence of lakes and large reservoirs, mean annual precipitation, geomorphology and *retention basins*). The choice of the regionalization method derived from a number of studies showing that the *topological kriging* is better than other, such as: *ordinary kriging*, *regressions* or the *region of influence* approach. This is because being this process an interpolation along the stream network it takes both area and the nested nature of the catchments into account. The flood information used in this thesis, in particular: average annual discharge, discharge with return periods of 30, 100 and 300 years were taken from the results obtained from the above mentioned project. It follows that the data to which the method is applied already take into account the actual presence of the dams: this quantitatively affects the value of the floods and ultimately the results we will obtain.

A key step within this thesis was the creation of the design flood wave to which the peak reduction is to be applied. In order to define this shape, it is necessary to have an additional parameter: the time constant, which is specific to each point in the river network. Information on this parameter is also available from the *HORA 3.0 project*.

In the validation phase of the method, the series on annual maximum discharge recorded at gauging stations in the analyzed catchments will be used: this information can be found within the *European database on floods* created and maintained over time by the *Institute of Hydraulic Engineering and Water Resources Management* of the *TU Wien*.

2.1.3 Data on dams

With regard to information on dams, the study refers to the *European database* managed by the *Institute of Hydraulic Engineering and Water Resources Management* of the *TU Wien*.

This dataset was created in recent years by grouping together information from *Public Administrations* and companies from all over Europe and combining, where available, information from the *GRanD database*.

This latter, the *Global Reservoir and Dam Database (GRanD)*, comes from the *Global Water System Project* which consists of an international collaboration to collect existing data on dams and reservoirs worldwide to provide the scientific community with a single uniform and reliable database.

Given the heterogeneity of the sources from which the information on dams were collected, the creation of this database required a careful control and verification phase to ensure that the result is as complete, reliable and current as possible.

Currently, a table is available for Austria listing all 78 large dams in the country with their main information: ID number, latitude and longitude, capacity, drainage area, main use and other uses (Annexes: Table 1).

2.2 Study area

This paper analyses the effect of large dams on floods by looking at a regional scale and specifically refers to the *Salzach* and the austrian part of the *Drau catchments* (Figure 2.1).

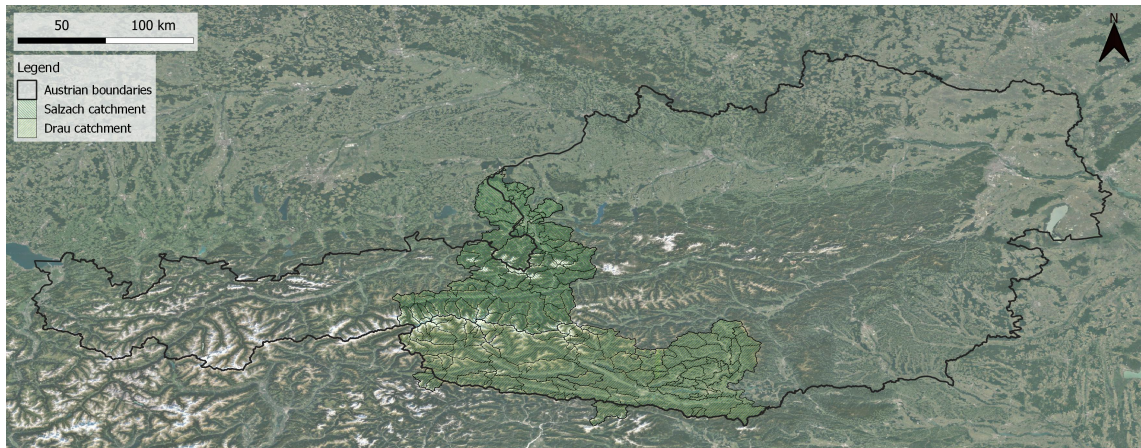


Figure 2.1: Study area

The *Salzach river* is the main river in the *Salzburg region*: it originates in the *Kitzbühel Alps*, more precisely on the *Salzachgeier*, defines for a part of its course the German border and finally flows into the *Inn* (Figure 2.2).

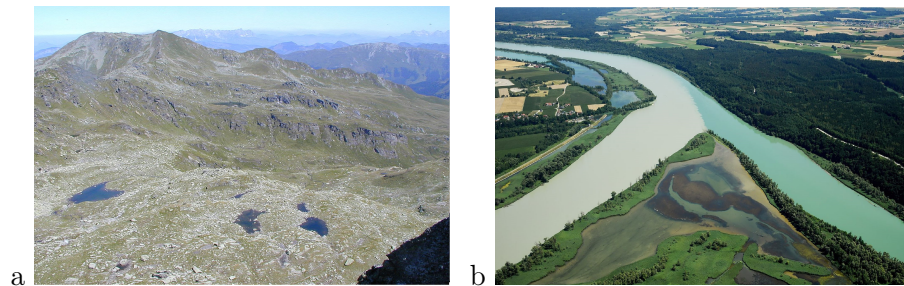


Figure 2.2: a: Source of the *Salzach river* (Wikipedia), b: *Salzach* and *Inn rivers* confluence (Wikipedia)

The *Drau river* is the second longest river in Europe: it has its source in *South Tyrol*, more precisely in the *Pusteria valley*, belongs only for a small part of its course to Austria and finally flows into the *Danube* near the border between Croatia and Serbia (Figure 2.3).



Figure 2.3: a: Source of the *Drau river* (Wikipedia), b: *Drau river* and *Danube river* confluence (Outdooractive)

Some additional information are listed Table 2.1 and Table 2.2.

river length	225 km
catchment area	6665 skm
source heigth	2300 m s.l.m.

Table 2.1: *Salzach river*

river length in Austria	210 km
catchment area	10397 skm
source heigth	1200 m s.l.m.

Table 2.2: *Drau river*

Both catchments are largely mountainous territories, characterized by the presence of the Alps: this topographic feature influences the climate system and, consequently, precipitation. In these alpine areas, runoff regimes are determined by glacio-nival characteristics, unlike in the lowlands where pluvial, hence rainfall-related, runoff regimes dominate.

It is for these more than appropriate topographical reasons that overall within the two basins are counted 27 of the 78 large dams in Austria, specifically 18 for the *Salzach basin* and 19 for the *Drau basin*.

These structures are mainly used for electricity production and only in a few cases for flood control (Annexes: Table 1): in fact, it should be remembered that hydropower accounts for about 70% of the total electricity production in Austria.

In heavily mountainous regions, such as those of interest, dams are located far upstream, within secondary and nested catchments. The two basins analysed (Annexes: Figure 1 and Figure 2), are related to two of the most important rivers in Austria: when considered in their entirety, moving from the source to the point where the basin closes, the dams within them are clearly combined in a complex manner.

Chapter 3

Methodology for flood peak reduction evaluation

In this work, a model was applied to study the intensity and evolution of the effect of dams on flood wave peak reduction. More precisely, the applied model follows the method used in the *HORA 3.0 project* aimed at the flood quantiles estimation in ungauged catchments (Figure 3.1).

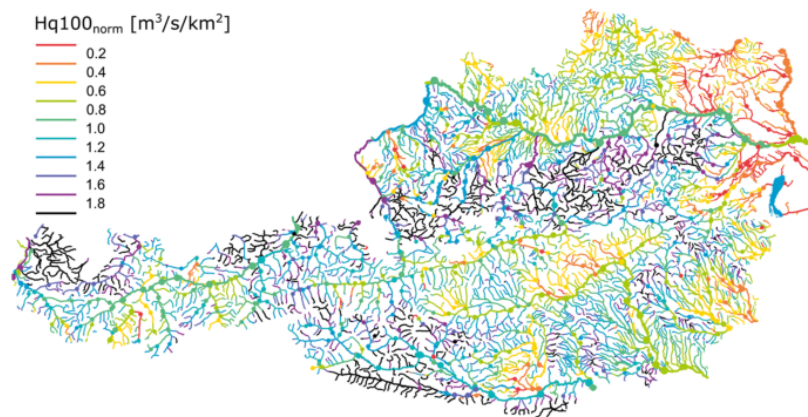


Figure 3.1: 100-year flood discharge (cm/s/skm) related to 100 skm, points show the values at the gauging stations while lines show the values regionalised to the river network (Blöschl et Al)

Although a study based on the analysis of series of data observed at gauging stations avoids including in the results uncertainties related to the assumptions of the method, in this context the aim is to produce a tool that can evaluate the reduction of the flood wave peak applicable, if desired, also in other contexts than that of the catchments under analysis and at a variety of return periods. Furthermore, it is emphasized that two other aspects are in favour of this work: (i) using this model it is possible to have results on a larger number of points than just the locations of the measurement stations and (ii) analyzing return periods of 100 and 300 years the evaluation of the peak reduction only from the observations at the measurement stations would have required the availability of sufficiently long data series, which in many cases are not available.

The steps listed below, the key components of the procedure generally mentioned in the first chapter of this thesis, were performed for each computation nodes in both analyzed catchments.

In the following chapter, the results are shown, discussed and interpreted, and in order to be comprehensive, as already mentioned, a validation and sensitivity analysis was carried out.

3.1 Selection of the computation nodes

In the *HORA 3.0 project*, have been evaluated the T-year floods in 21730 ungauged catchments using the first three statistical moments available for the 782 gauged catchments across Austria.

Through the results of this previous work, having identified the catchments for our analysis, the nodes defined in the context of the *HORA 3.0 project*, were selected: for each of them the effect of the dams was subsequently evaluated (Annexes: Figure 1 and Figure 2).

The Table 3.1 shows the information available at each of these calculation nodes.

Information	Units
ID numer	[-]
area upstream	[skm]
discharge values for a return period of 30,100 and 300 years	[cm/s]
mean annual discharge	[cm/s]

Table 3.1: Information available at each node

3.2 Representative dam definition

Within both analyzed watersheds there are numerous dams, which, proceeding from upstream to downstream along the catchment network, combine in a complex way giving a different effect depending on the location of the calculation nodes. In order to account at any point for all the dams located upstream, a *representative dam* with equivalent drainage area and storage volume is substituted for them.

Following the method used for *retention basins* in the *HORA 3.0 project*, three different combination cases were considered: the series configuration, the parallel configuration and their combination (Figure 3.2).

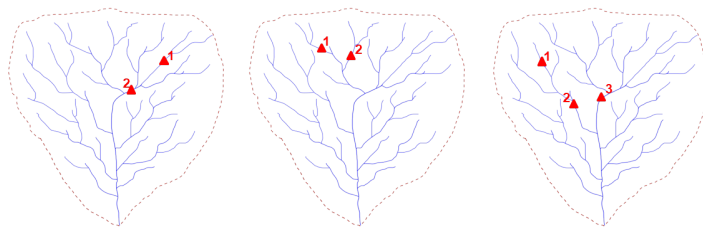


Figure 3.2: *Representative dam*

In the case of computation nodes with at most two upstream dams the *representative dam* will be the series or parallel combination of the two, while in the case of computation nodes with more than two upstream dams the definition of the *representative dam* is obtained by an iterative process. The two most upstream dams of all those considered are taken into the analysis at the first step and the *representative dam* is calculated for them, this is then combined in series or in parallel with the next dam obtaining another new *representative dam*: this process is repeated until all the dams have been incorporated.

The Table 3.2 below shows the formulas applied for the calculation.

If the dams are located in series, i.e. along the same river branch, then the volume will simply be the sum of the volumes of the dams upstream of the calculation node considered. Following each confluence, i.e. dams combined in parallel, on the other hand, the value of the available volume will also depend on the area drained by the dams: being the formula a weighted average, with the protected area, of the various volumes.

Dams characteristic	In series	In parallel
Volume	$V = V_{D1} + V_{D2}$	$V = \frac{V_{D1} \cdot PA_{D1} + V_{D2} \cdot PA_{D2}}{PA_{D1} + PA_{D2}}$
Protected area	$PA = \frac{PA_{D1} \cdot V_{D1} + PA_{D2} \cdot V_{D2}}{V_{D1} + V_{D2}}$	$PA = PA_{D1} + PA_{D2}$

Table 3.2: *Representative dam* volume and protected area

3.3 Effective volume available for flood control

The large dams which are analyzed in this work are aimed at power generation, which is precisely why the volume available at the time of flood arrival is not, unlike *retention basins* analysed in the *HORA 3.0 project*, the total volume but only a percentage of it.

The actual volume available for flood control is not a value that can be taken as constant.

In fact it is clearly related to the seasonality of the flow rate and the rules of use of the

dams.

In general, greater flood peak reduction is available if operation rules would be adopted to explicitly guarantee a free volume for flood control. Moreover this goal would not be so difficult to achieve since most hydropower companies have hydrologic models driven by precipitation and temperature forecasts available and thus anticipatory preparation could actually be accomplished. However, unfortunately these operations are inconsistent with the goal of maximizing energy production and are not provided for in any technical regulations. Also diversions and inter-basin water transfer can provide a difference in the available volume at the dams, but in our analysis, as with the rules of use of the dams, these procedures are not taken into account.

The fraction of volume that can be used to store water during an event is also linked to the floods timing and the hydrological conditions of the river network. As identified by Blösch et Al (2017): ongoing climate change is the reason for a change in floods timing (Figure 3.3). In particular regarding the study area of this thesis, the results show that warmer temperatures lead to earlier spring snowmelt floods: it follows that the capacity of the dams will also be different over the years.

Since we could not know the managing rules and we are focusing on a general analysis, a percentage of the total storage volume of 30% was assumed.

3.4 Regionalization of the time constant

For each node, the initial step is to construct the design flood wave to which the peak reduction will be applied. To define this shape it is necessary to know a parameter which describes the flood event duration: the time constant, which needs to be specified in each point of the river network.

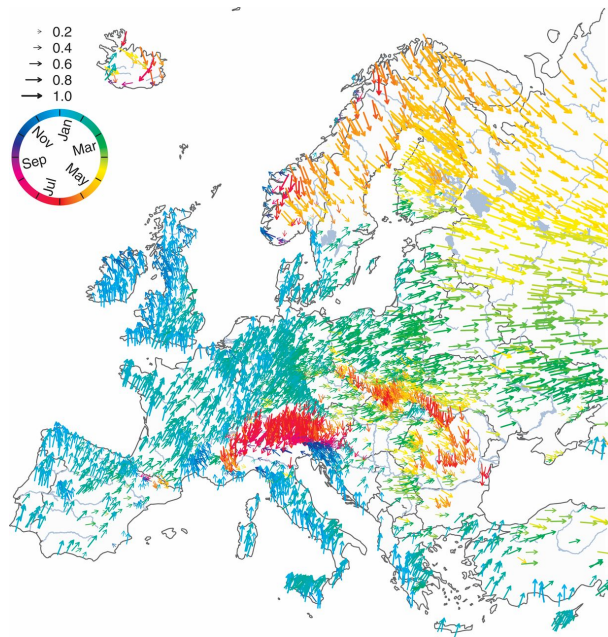


Figure 3.3: Observed average timing of river floods in Europe, 1960–2010 (Blöschl et Al)

The values (Annexes: Figure 3) of this constant were calculated using a *Matlab code* made available by the *Institute of Hydraulic Engineering and Water Resources Management* of the *TU Wien*. This algorithm allows time parameters t_c to be calculated by the daily and maximum annual discharges available at the gauging stations.

The timescale parameter t_c is *the time of concentration* that is the time required for runoff to travel from the hydraulically most distant point in the catchment to the outlet: it can be represented by the ratio of the volume V_Q of a flood wave and its peak discharge Q_s (Figure 3.4).

In the work of Merz, Blöschl and Piock-Ellena (1999) on the *Gradex method*, the parameter r is introduced, to which the *the time of concentration* is closely related, which is defined as the ratio of the peak discharge Q_s to Q_{mH} that is the average flow rate over a reference period H (Figure 3.4).

Both of these two factors summarize the dynamics of runoff and are inversely proportional to each other. Small values of t_c occur for events of short duration or for areas with a rapid

runoff response that produce a thin wave with a relatively large peak. Conversely, large values of t_c occur with long duration events or for areas with a slow response to runoff characterized by a flat wave with a relatively small crest and temporally balanced rainfall distribution.

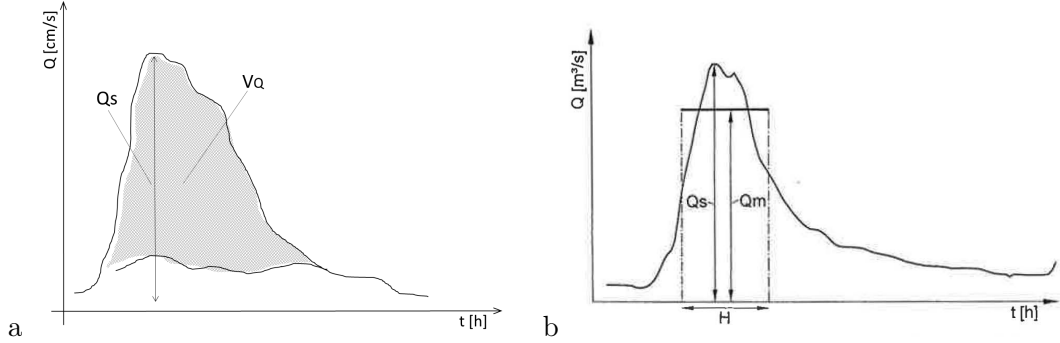


Figure 3.4: a: Calculation of the t_c value, b: Calculation of the r value (Merz et Al)

The formulas for calculating these parameters are shown in Table 3.3.

Parameter	Units
$r = \frac{Q_s}{Q_m H}$	[-]
$t_c = \frac{V_Q}{Q_s}$	[h]

Table 3.3: Formulas for calculating r and t_c

As can be seen in Annexes: from Figure 1 to Figure 3, the points for which the t_c parameter is known do not coincide with the calculation nodes: to know its value everywhere a regionalization was applied through *ordinary kriging* available in *QGIS software*.

Kriging is a regression method used in spatial analysis to interpolate the value of a quantity at one point in space by knowing its value in other points. In *kriging* this spatial interpolation is based on the *autocorrelation* (the degree of dependence between the values assumed by a sampled function in its domain) of the quantity, assuming that it varies in space with continuity. Different types of *kriging* can be found: among these we can find

the *ordinary kriging*. This method uses an average of a subset of neighbouring points to produce a particular interpolation point and relies on the spatial correlation structure of the data to associate weighting values with them, the sum of which must equal unity.

In Figure 3.5 we can see the experimental *semivariogram* and the theoretical *semivariogram* that best approximates the former. The *semivariogram* is a graph that relates the distance between two points and the *semivariance* value between the measurements taken at these two points. Having this trend we can deduce that the data are correlated up to a certain maximum distance where the function tends to become horizontal.

Figure 3.6 and Figure 3.7 shows that, as we expected, t_c values increase downstream.

In this work, a unique t_c value was considered for each return period. This assumption may not be verified being that the evolution of flood events and the response of a catchment to it, are elements that vary according to the magnitude of the event and thus to its return period.

3.5 Design hydrograph creation

The design flood wave used in this method follow an analytical *Gamma form* and it is defined by three values: the time constant t_c , the peak discharge HQT and the mean annual discharge MQ . The latter is the mean of daily discharge values of equal intervals (e. g. month, half-year, year) in the defined period and is considered here as the statistically most probable starting value for the flood wave. The shape of the design flood wave needs, to be evaluated, two auxiliary parameters: the *scale parameter* θ and the *time to peak* t_{peak} at which the maximum discharge is registered.

These two parameters and the design flood wave are defined by the equations shown in Table 3.4.

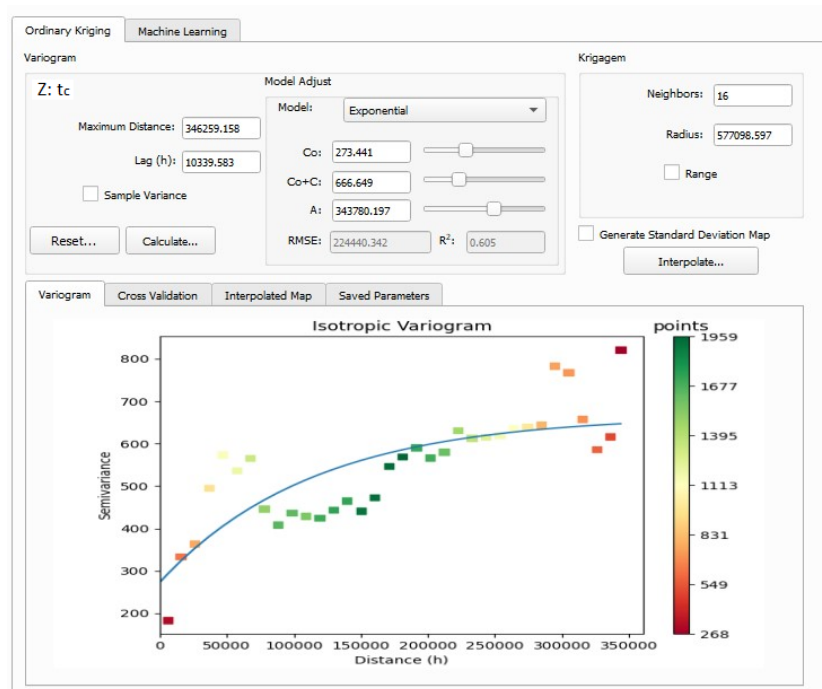


Figure 3.5: Settings of the *kriging* applied to the t_c values

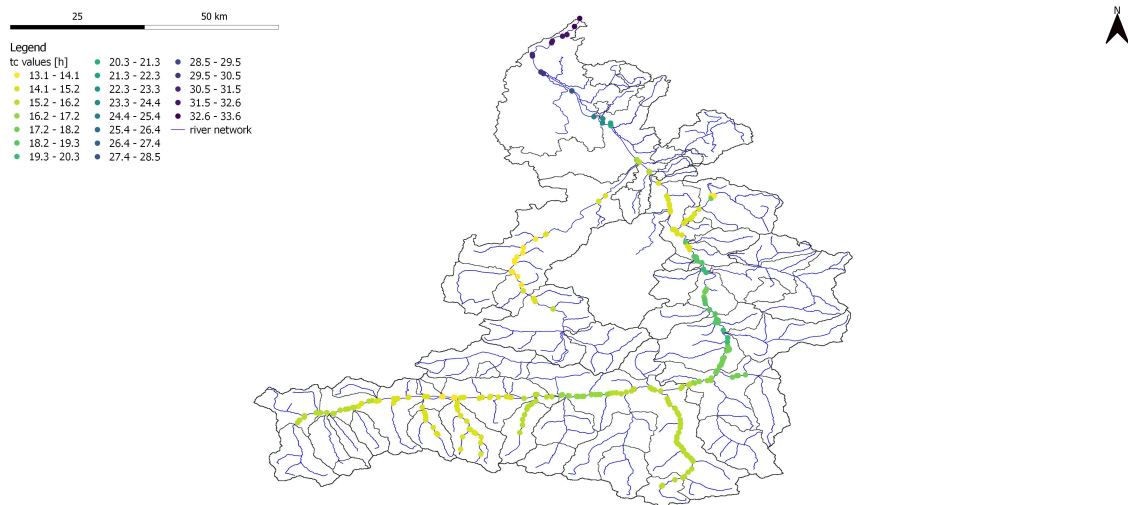


Figure 3.6: Time constant values for each computation node of the *Salzach catchment*

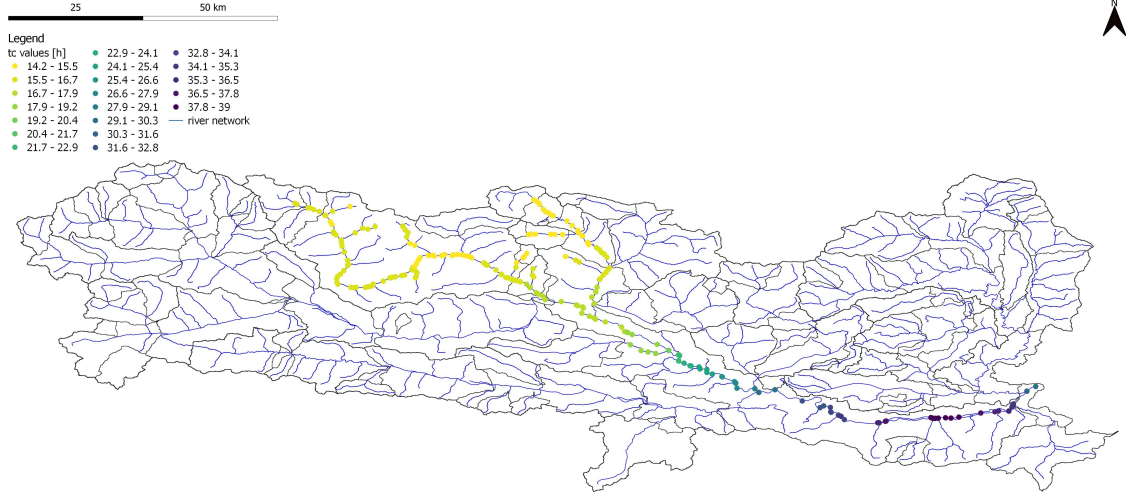


Figure 3.7: Time constant values for each computation node of the *Drau catchment*

In this step three different flood waves were defined for every calculation node: each of these has the same mean annual discharge and time constant but different peak discharges referring to the return periods of 30, 100 and 300 years (Figure 3.8).

$$\theta = 0.224418 \cdot t_c \cdot \left(1 + \left(\frac{MQ}{HQ} \right)^{1.09} \right)^{1.35}$$

$$t_{peak} = 3 \cdot \theta$$

$$Qt = MQ + (HQ - MQ) \cdot \left(\frac{e \cdot t}{t_{peak} P} \right)^3 \cdot e^{-\frac{t}{\theta}}$$

Table 3.4: Design hydrograph parameter and equation

3.6 Protection ratio calculation

The flood wave reduction, described in the last section of this chapter, is not performed on the total hydrograph but only on the protected portion of it (Figure 3.9). This means that only the fraction of the curve that competes with the dams is modified.

In order to obtain the protected hydrograph, the flood wave must be split into two components, and this is done by introducing a coefficient called the *protection ratio PR*, which must be multiplied by each hydrograph value. This, as shown in Figure 3.10, represents

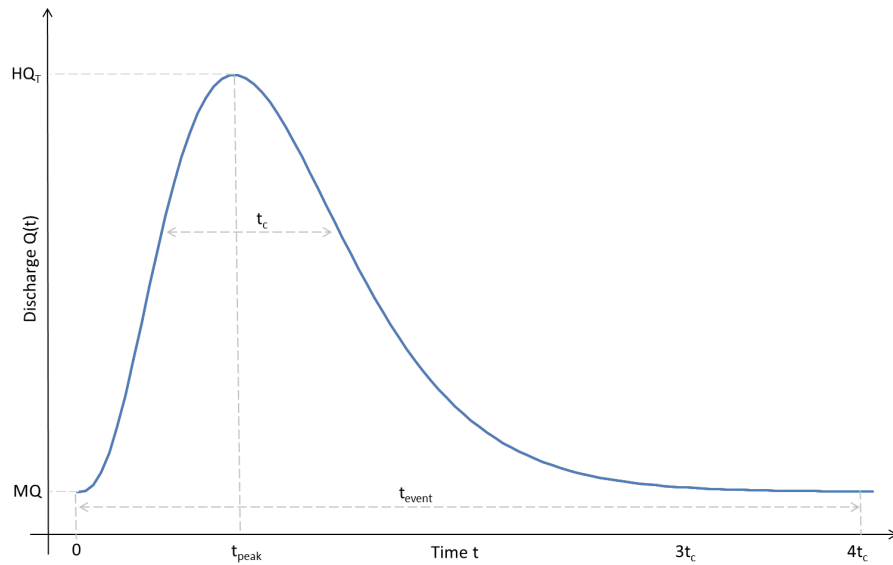


Figure 3.8: Analytical *Gamma form* for the design flood wave

the ratio of the area drained by the dam, or of the set of dams, to the area upstream of the calculation point: therefore, it is a parameter that must be calculated for each computation node. By definition, this ratio is always a number between 0 and 1 and has a decreasing trend as we move downstream along the river network.

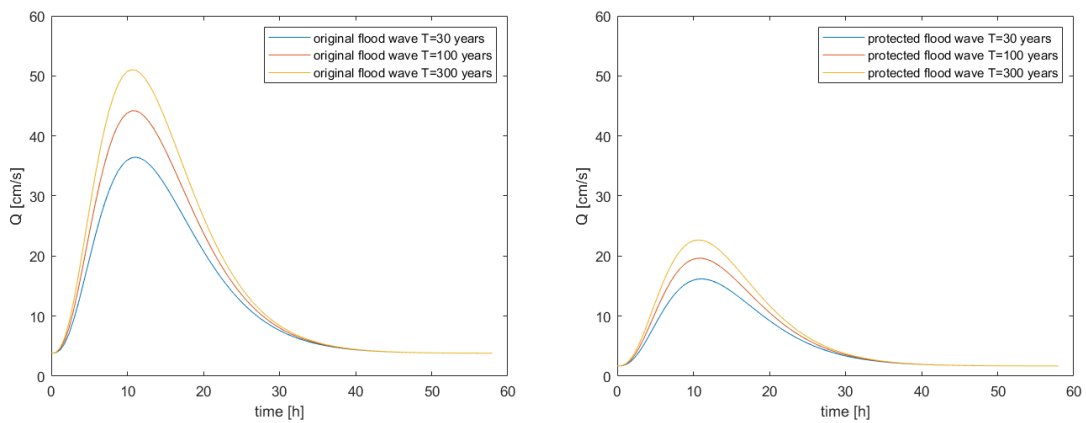


Figure 3.9: Original and protected flood wave

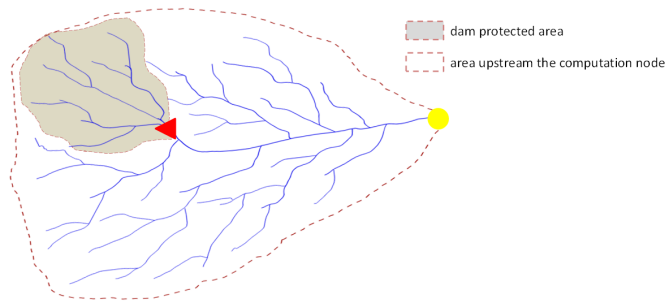


Figure 3.10: *Protection ratio*

3.7 Filling discharge definition

The flood wave storage mechanism and thus the peak reduction routine, begins only from the moment when the discharge at the point of analysis is greater than the so-called *filling discharge*. This value is therefore a key piece of information in the model and is specific to each dam since it depends on the dam's usage rules.

A *filling discharge* value that is too small is not suitable because the reservoir in this case would start storing too early and thus fail to reduce at the actual time of need since the available volume at that point is already partly occupied. Conversely, a too high *filling discharge* value does not take advantage of the full availability of the reservoir.

For the calculation the relationship given in the *HORA 3.0 project* and shown in Table 3.5, was applied. To defined this formula additional information concerning the efficiency of the *retention basins* in reducing discharges with a return periods of 100 years, was used. As the retention volume of some basins was known, the efficiency was used to back-calculate the *filling discharge* for them and subsequently, a single regression model was built to model the relationship.

$$Q_{filling} = MQ_{protected} + \frac{Q_{100_{protected}} + MQ_{protected}}{2.66}$$

Table 3.5: Equation for the *filling discharge*

3.8 Application of the peak reduction routine

This routine consists of a flood wave transformation, by which each flood wave is reduced by a certain amount indicated as the percentage of reduction of the flood wave peak.

The reduction occurs as follows: (i) when the *filling discharge* is reached this value is linked to the peak discharge, (ii) then the *representative dam* volume is compared with a portion of the flood event volume, the light-blue area in Figure 3.11: if it is bigger a new peak for the hydrograph is considered moving along the falling limb, (iii) now this new portion of the flood event volume is again compared with the *representative dam* volume and if it is smaller, the process is repeated. The explained procedure is repeated until the portion of the flood event volume at the *i-th iteration* is equal to the *representative dam* volume.

Four different situations can occur: (i) the hydrograph, or better the portion that is within the competence of the *equivalent dam*, is not reduced because the discharge is not large enough to start storage in the dams, (ii) the flood wave is not reduced because the dams does not have a volume large enough, (iii) the hydrograph is partially reduced because dams cannot accumulate the entire volume of the flood event and finally (iv) the flood wave is totally reduced.

Anyway the reduced peak discharge can range between the original peak discharge and the *filling discharge*.

As mentioned before this procedure is applied to the protected portion of the flood wave, so once the reduced hydrograph has been derived it must be combine, through a simple

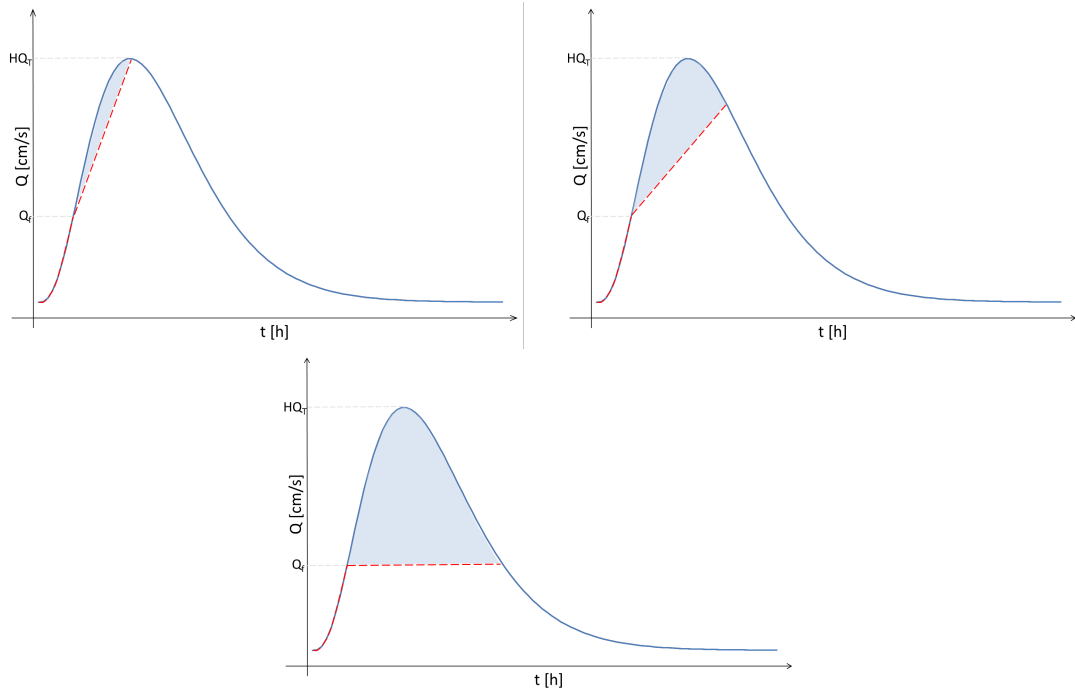


Figure 3.11: Flood wave transformation

vector sum, with the unprotected portion, which has not been modified, to derive the final flood wave to be compared with the original one.

The Table 3.6 shows how the percentage of reduction of the peak is evaluated at each computation node.

For the purpose of this work, the effect of the dams is evaluated only in terms of peak reduction and not in terms of volume and transformation of the input flood wave, or the duration of the event, as for example analysed by Manfreda et Al (2021).

$$\%R = \frac{peak_{reducedfloodwave} - peak_{originalfloodwave}}{peak_{originalfloodwave}}$$

Table 3.6: Percentage of peak reduction

Chapter 4

Flood peak reduction for design event and comparison to observation

This chapter presents the results obtained from the application of the peak reduction method, on a case-by-case basis, with a brief discussion aimed at justifying and interpreting the values obtained.

In addition, the validation and sensitivity analysis performed for some nodes in both basins are detailed here.

4.1 Information at each calculation nodes

Through the steps described in the previous chapter, the quantities shown in Table 4.1 are available for each calculation point, in addition to the information shown in Table 3.1.

Information	Units
$V_{\text{representative dam}}$	[cm]
$PA_{\text{representative dam}}$	[skm]
t_c	[h]
t_{event}	[h]
Q_{filling}	[cm/s]
protection ratio	[-]
R_{peak}	[%]
$R_{\text{evolution 30-100 years}}$	[%]
$R_{\text{evolution 100-300 years}}$	[%]

Table 4.1: Information available at each node

The percentages of reduction of the flood wave are represented below from Figure 4.1 to Figure 4.10 (for more details see Annexes: from Figure 4 to Figure 19).

Some initial conclusions can be drawn from the figures below, which only describe the results obtained in a general way: there are of course exceptions to this overall trend which are discussed in detail in the next section.

In general, it can be seen that the percentage of peak reduction, as we expected, has a decreasing trend moving from upstream to downstream along the river network. The effect is very pronounced at the calculation nodes right downstream of the dams and then decreases until it becomes insignificant for the nodes which are located on the main rod under analysis.

Considering the transition from 30 to 100 years and from 100 to 300 years, for the majority of the nodes in which the percentage of reduction is significant, this increases implying that in these contexts dams can be effective for phenomena of greater intensity.

For the *Salzach catchment*, the percentage of reduction reaches maximum values of: 40% for flood waves with a return period of 30 years, 47% for flood waves with a return period of 100 years and 52% for flood waves with a return period of 300 years.

With regard to the *Drau catchment*, the percentage of reduction reaches maximum values

of: 53% for flood waves with a return period of 30 years, 67% for flood waves with a return period of 100 years and 74% for flood waves with a return period of 300 years.

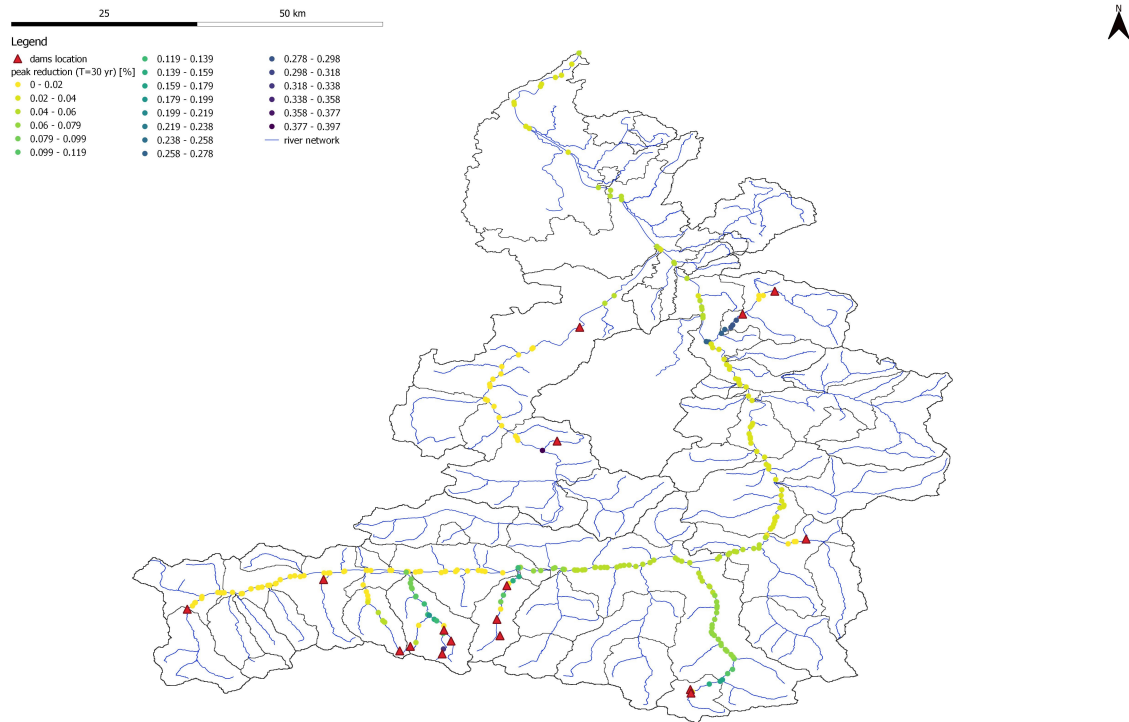


Figure 4.1: Percentage of peak reduction for (T=30 yr) for the *Salzach catchment*

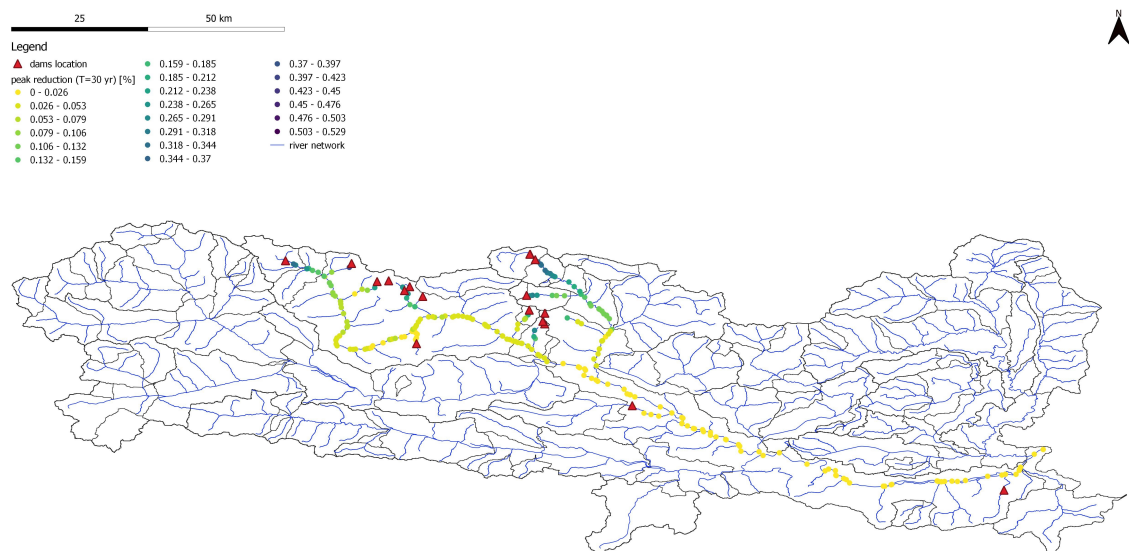


Figure 4.2: Percentage of peak reduction for (T=30 yr) for the *Drau catchment*

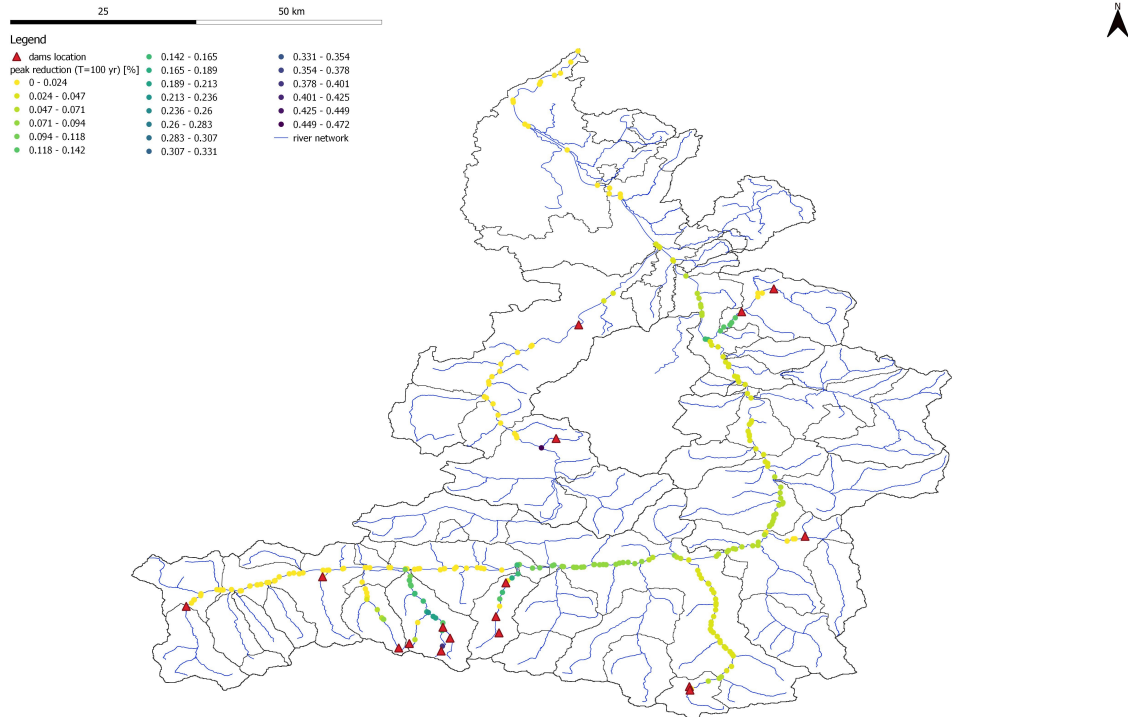


Figure 4.3: Percentage of peak reduction for (T=100 yr) for the *Salzach catchment*

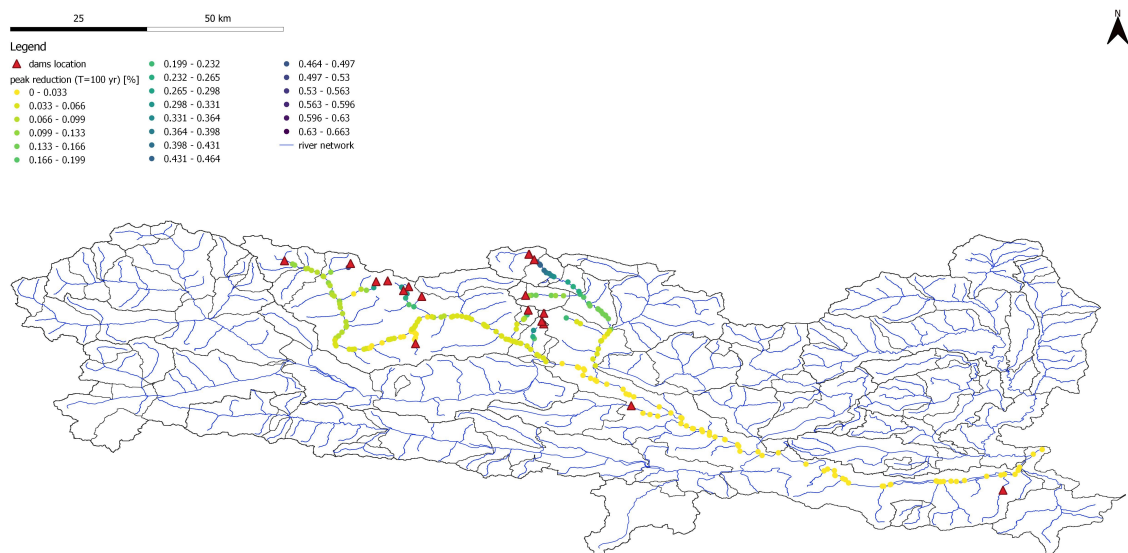


Figure 4.4: Percentage of peak reduction for (T=100 yr) for the *Drau catchment*

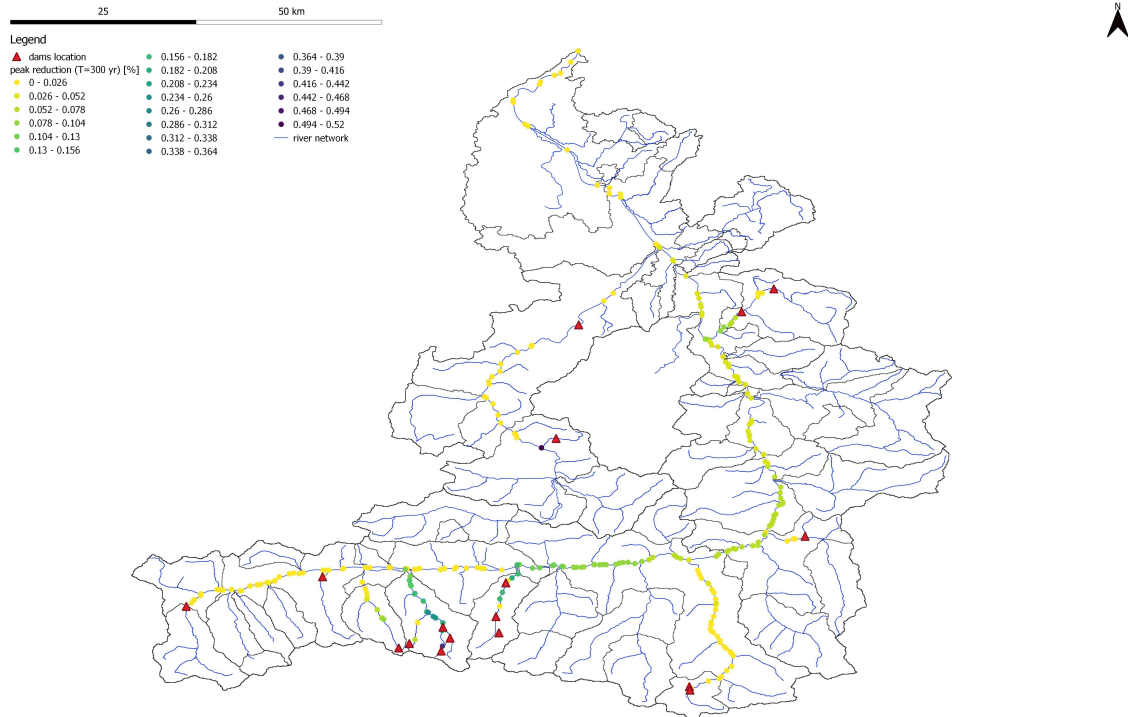


Figure 4.5: Percentage of peak reduction for ($T=300$ yr) for the *Salzach* catchment

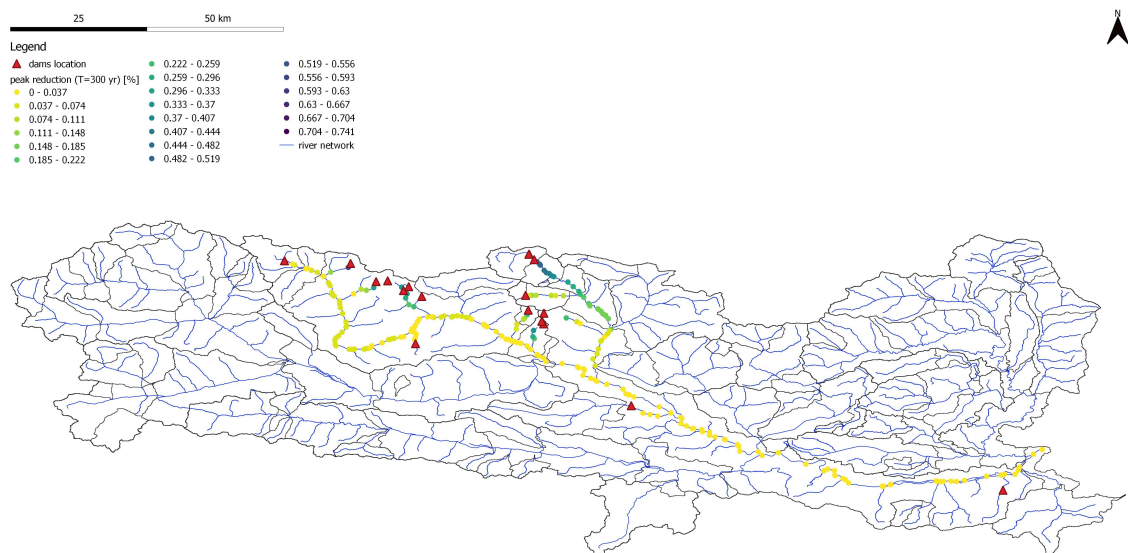


Figure 4.6: Percentage of peak reduction for ($T=300$ yr) for the *Drau* catchment

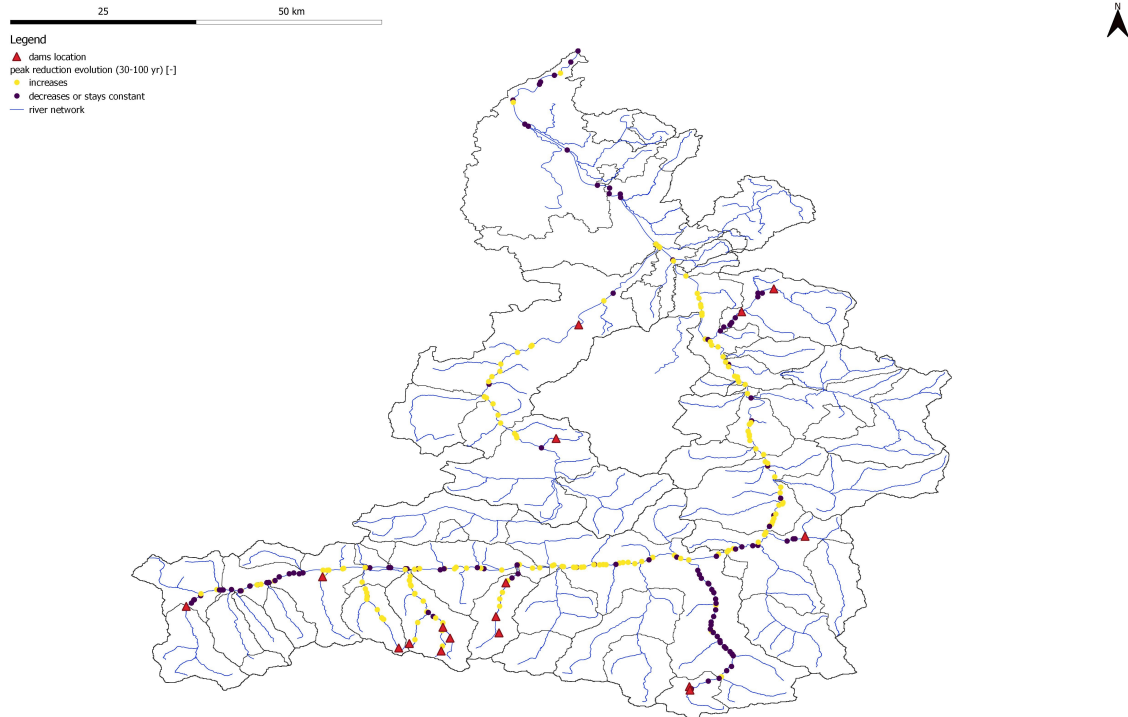


Figure 4.7: Evolution of the peak reduction (from 30 to 100 yr) for the *Salzach catchment*

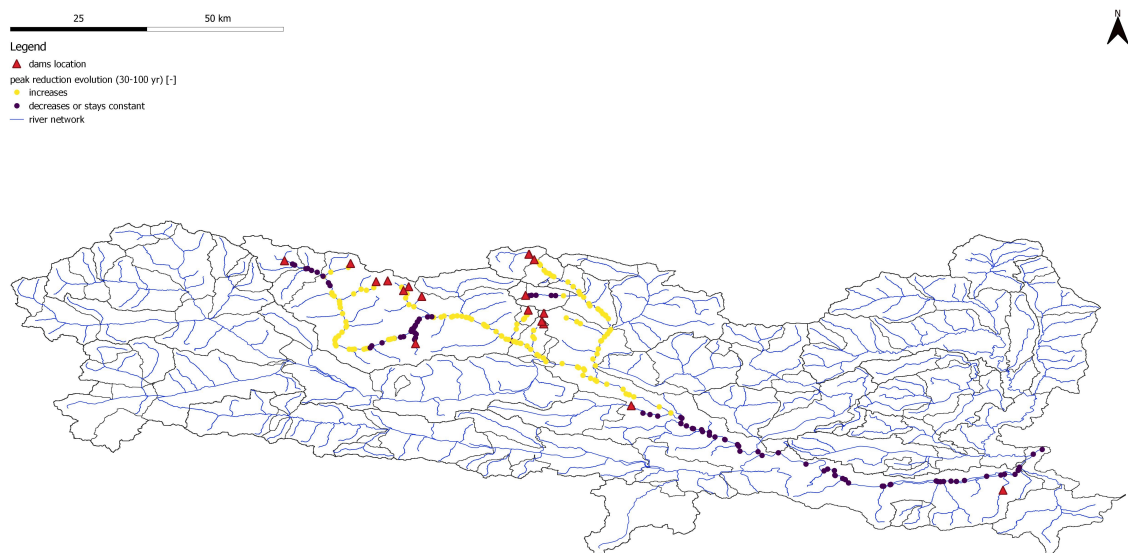


Figure 4.8: Evolution of the peak reduction (from 30 to 100 yr) for the *Drau catchment*

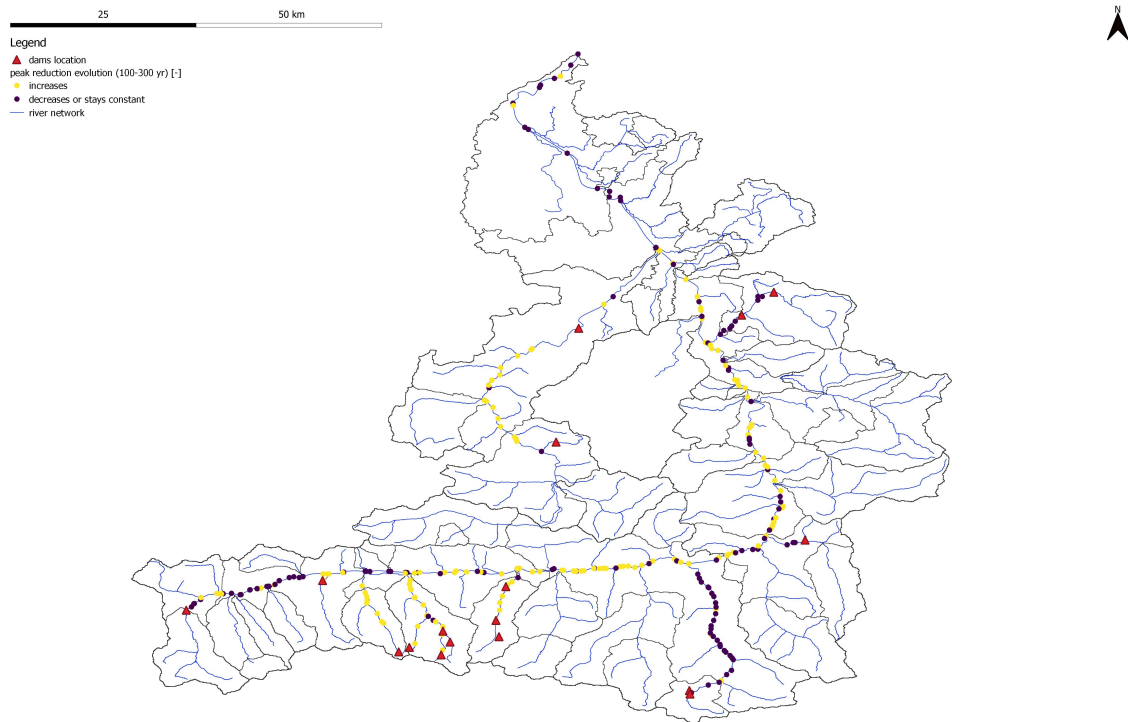


Figure 4.9: Evolution of the peak reduction (from 100 to 300 yr) for the *Salzach catchment*

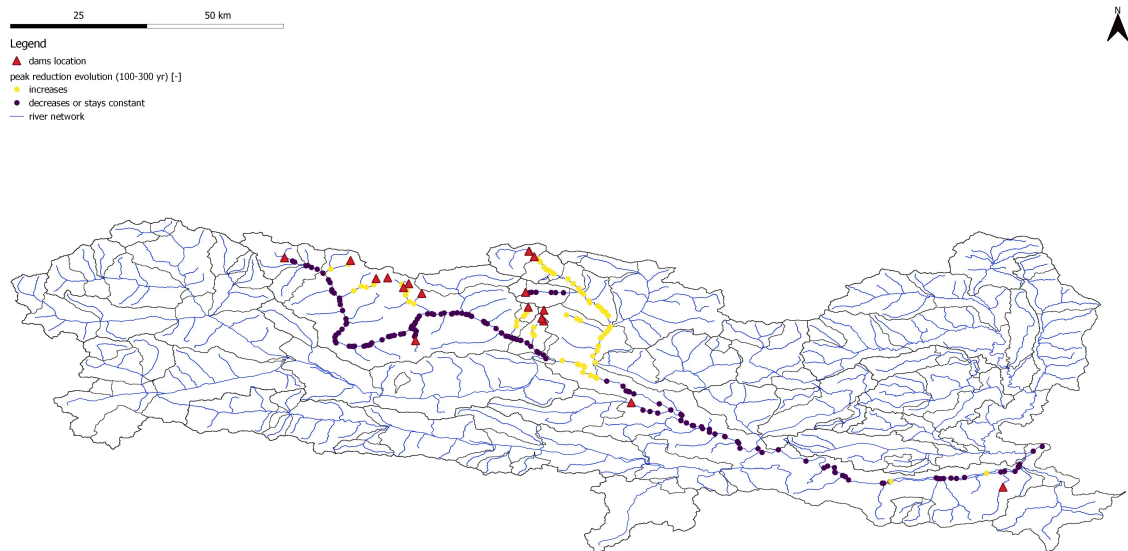


Figure 4.10: Evolution of the peak reduction (from 100 to 300 yr) for the *Drau catchment*

4.2 Result discussion

From the simulations performed, we obtained the percentage of peak reduction for each node along the hydrographic networks under analysis (Annexes: Table 2 and Table 3). We can have three different case: (i) the percentage of peak reduction increases with the return period since the volume is large enough and storage can be continued even with larger events; (ii) the percentage of peak reduction decreases with the return period since the dam is more effective with smaller events; (iii) and the percentage of peak reduction is zero in the case of insufficient volume or flood not big enough to start the storage procedure. The first case predicts an increase in the percent of peak reduction with return periods, such as in Figure 4.11, Table 4.2 and Figure 4.12. This condition is motivated by the fact that dams, being by definition large, have enough volume to reduce not only an event with a 30 years as return period but also 100 and 300 years as return periods.

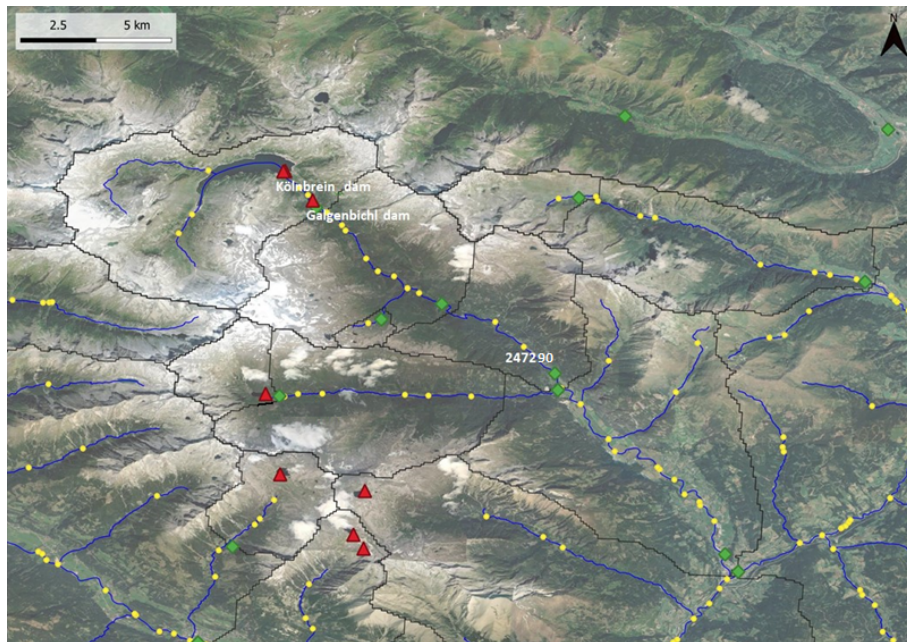


Figure 4.11: Location of the analysed computation node

%R30	%R100	%R300
-0.190	-0.233	-0.260

Table 4.2: Percentage of peak reduction (computation node 247290)

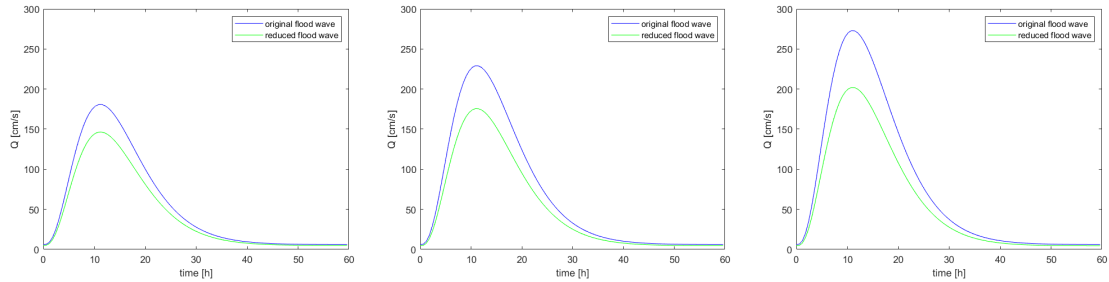


Figure 4.12: Original and reduced floodwave with a return period of 30, 100 and 300 years (computation node 247290)

As an example of the second case study we reported here the situation shown in Figure 4.13, Table 4.3 and Figure 4.14. As can be seen in this case the peak reduction decreases with return period, showing that the *representative dam* upstream of the node under analysis works well for smaller return periods.

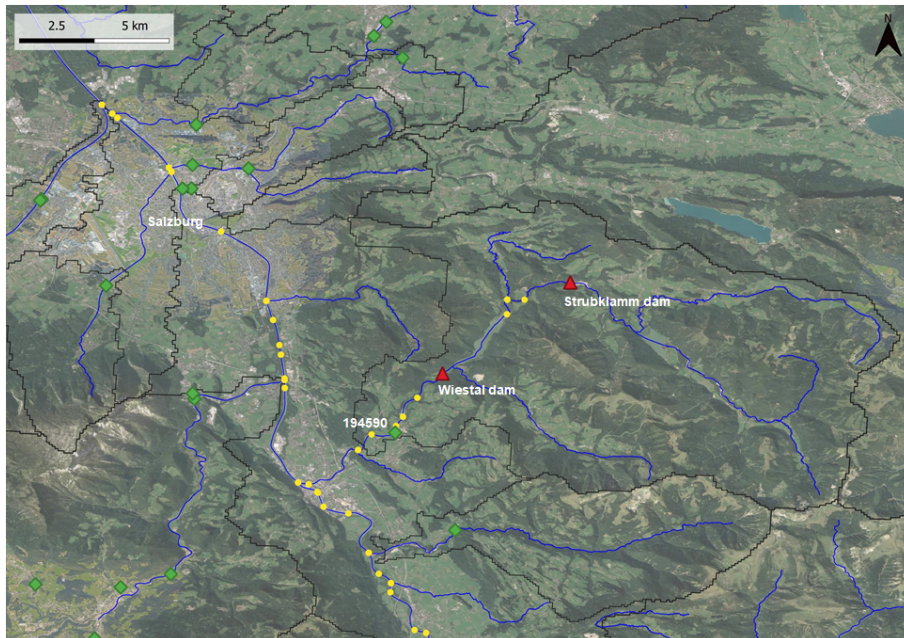


Figure 4.13: Location of the analysed computation node

%R30	%R100	%R300
-0.259	-0.124	-0.100

Table 4.3: Percentage of peak reduction (computation node 194590)

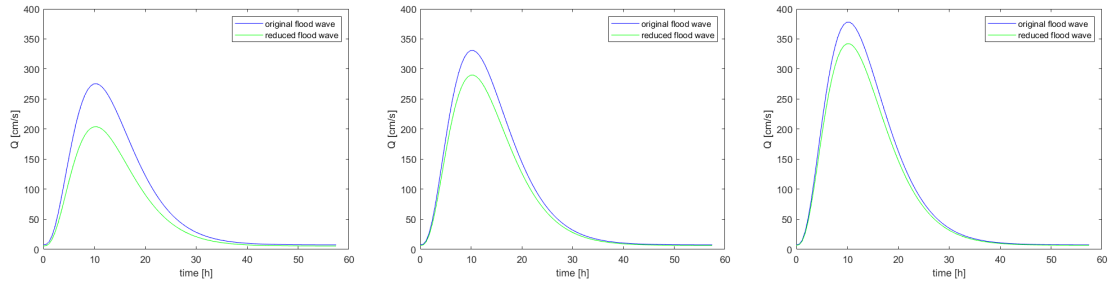


Figure 4.14: Original and reduced floodwave with a return period of 30, 100 and 300 years (computation node 194590)

To prove this, an analysis of the percentage of peak reduction for different return periods was detailed, in addition to the three analyzed throughout the project. As can be seen in Table 4.4 and Figure 4.15 the percentage of peak reduction has a maximum for the return period of 5 years.

$Q_{2_{pre}}$	$Q_{5_{pre}}$	$Q_{10_{pre}}$	$Q_{30_{pre}}$	$Q_{100_{pre}}$	$Q_{300_{pre}}$
120.920	182.106	220.560	275.724	331.159	378.285
%R2	%R5	%R10	%R30	%R100	%R300
-0.300	-0.422	-0.261	-0.259	-0.124	-0.100
$Q_{2_{post}}$	$Q_{5_{post}}$	$Q_{10_{post}}$	$Q_{30_{post}}$	$Q_{100_{post}}$	$Q_{300_{post}}$
84.650	105.208	162.905	204.312	290.095	340.456

Table 4.4: Dam functioning for different return period

This can also be understood by looking at the graph in Figure 4.16, where the pre- and post-dam *flood frequency curves FFCs* are shown and is possible to see the *S-shape* of the latter indicating that the *representative dam* is more effective for a certain return period in particular.

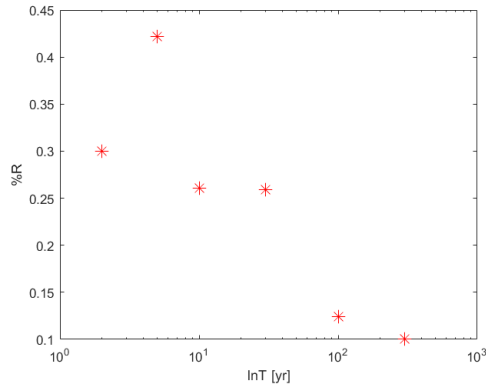


Figure 4.15: Percentage of peak reduction for different return periods

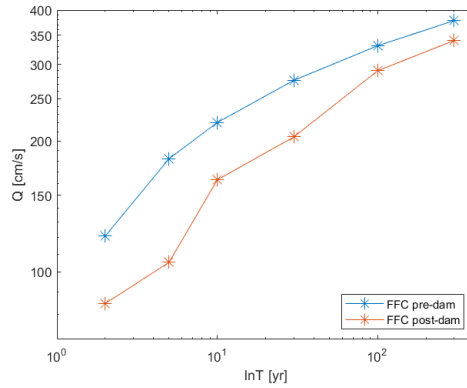


Figure 4.16: Flood frequency curves pre- and post-dam

For the condition depicted in Figure 4.17, Table 4.5 and Figure 4.18, it can be seen that in this case the percentage of the peak reduction is zero for each of the return periods under analysis. Going into the details of the calculation routine, this result is due to an available volume too small to accumulate and thus have an effect on the flood wave.

%R30	%R100	%R300
0.000	0.000	0.000

Table 4.5: Percentage of peak reduction (computation node 239690)

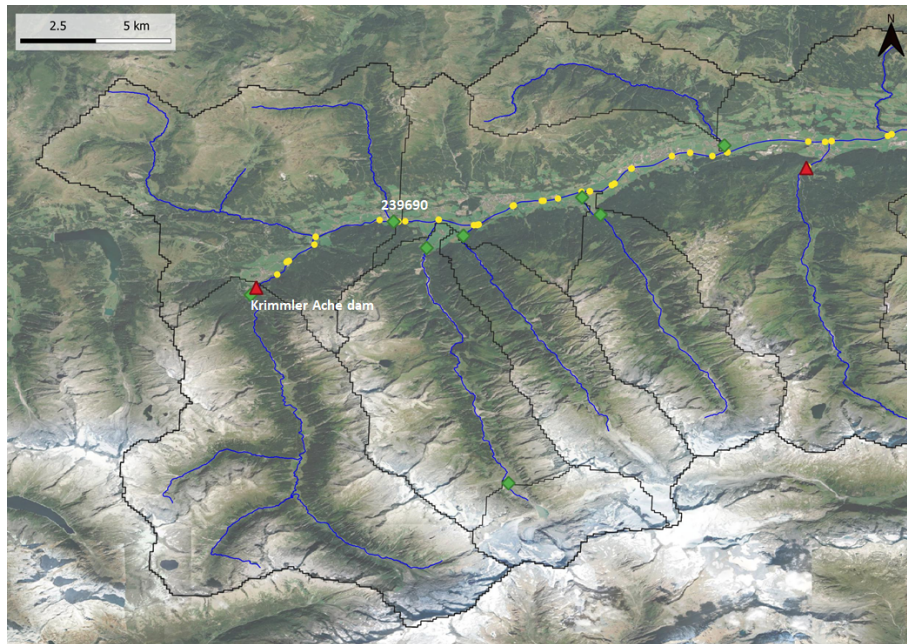


Figure 4.17: Location of the analysed computation node

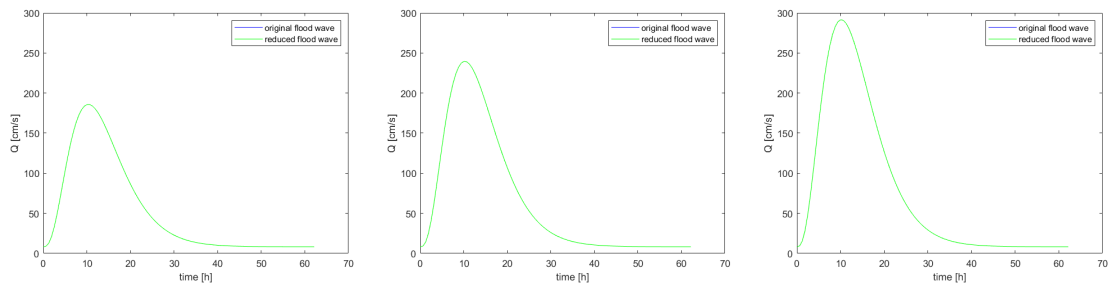


Figure 4.18: Original and reduced floodwave with a return period of 30, 100 and 300 years (computation node 239690)

The condition for which the peak is not reduced may also be related to a *filling discharge* value higher than the peak of the flood wave, in other words, the magnitude of the event is not high enough to initiate the process of peak reduction. This condition never happened in our simulations and this because we are studying huge events, with return periods of 30, 100 and 300 years.

4.3 Comparison with literature

In general, our results, have been encountered in the literature

In particular the evolution in space of the percentage of reduction is reflected in Bertola et Al (2019): according to this project the big dams that are built for hydroelectricity purposes, have no significant flood attenuation at the gauging stations because these effects are mainly local.

Stecher and Herrnegger (2022), while providing higher *flood peak reduction* results, emphasise in their work a clear trend of decreasing *FPR* moving downstream, particularly pronounced immediately after the confluence of tributaries (Figure 4.19 and Figure 4.20). Considering return periods, their results indicate that events with return periods of more than 30 years show a significant reduction in flood peaks, with an average of more than 33% (Figure 4.21).

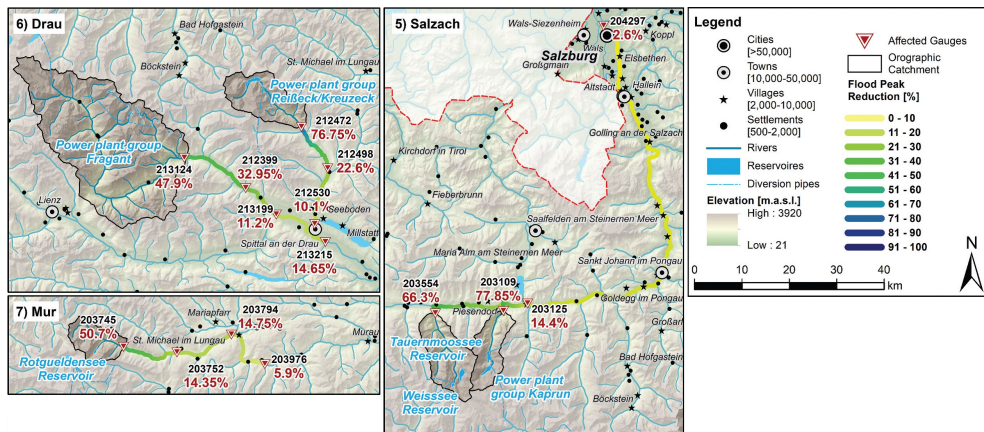


Figure 4.19: Median *flood peak reduction* (Stecher and Herrnegger)

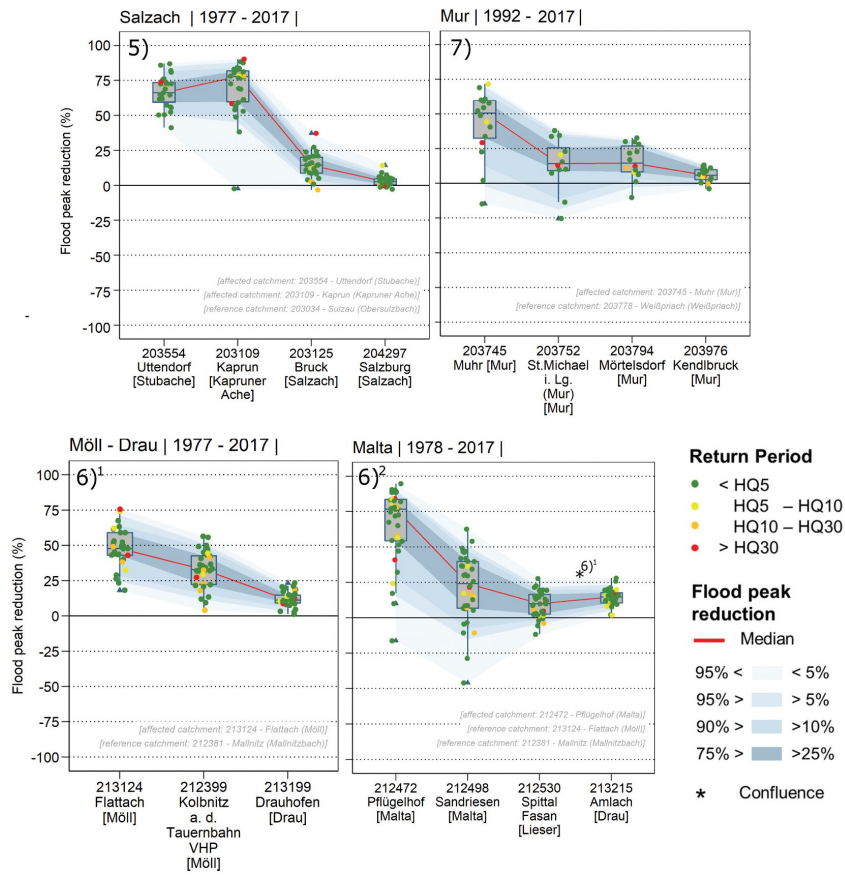


Figure 4.20: Event-based *flood peak reduction* and return periods at gauges affected by hydropower reservoirs (Stecher and Herrnegger)

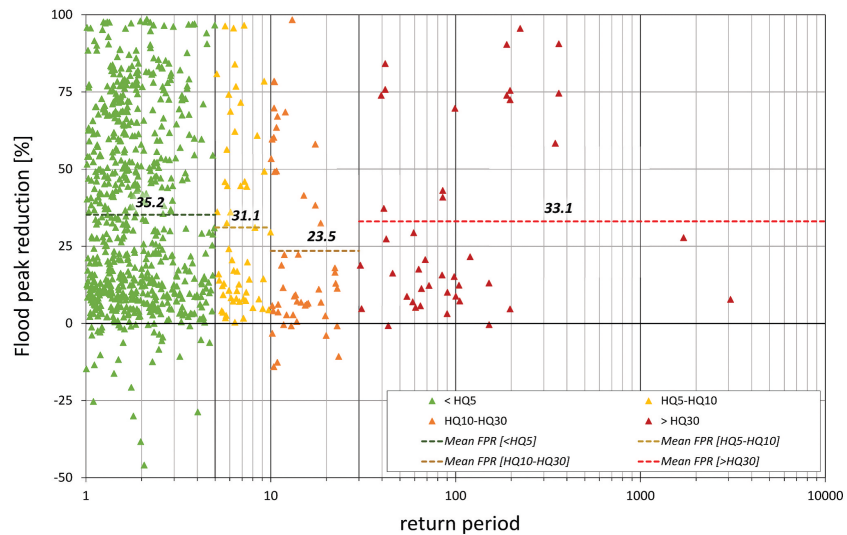


Figure 4.21: Relationship of return periods and the *flood peak reduction* (Stecher and Herrnegger)

4.4 Results validation

The results obtained have been validated both in space and in time considering the information coming from the gauged stations available in the catchments.

The analysis carried out in this thesis work applies a computational routine to evaluate flood wave peak reduction: using a model, it is necessary to evaluate its performance and, later, its applicability, through validation.

Figure 4.22 and Figure 4.23, shown gauging stations and computational nodes used for validation.

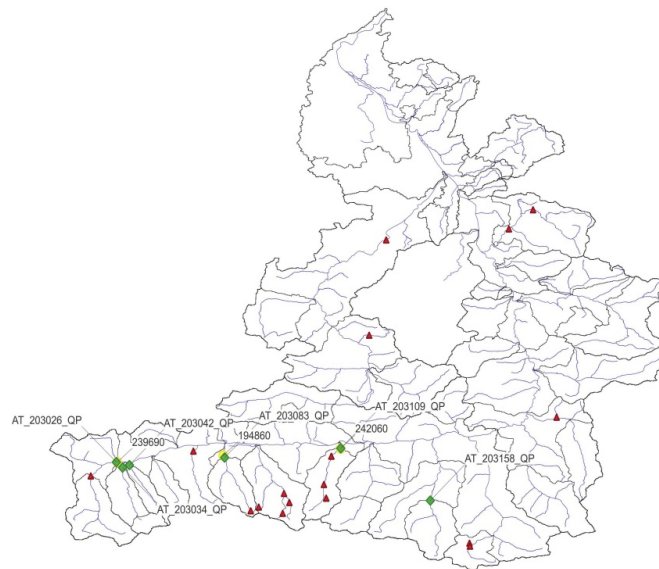


Figure 4.22: References for validation in the *Salzach catchment*

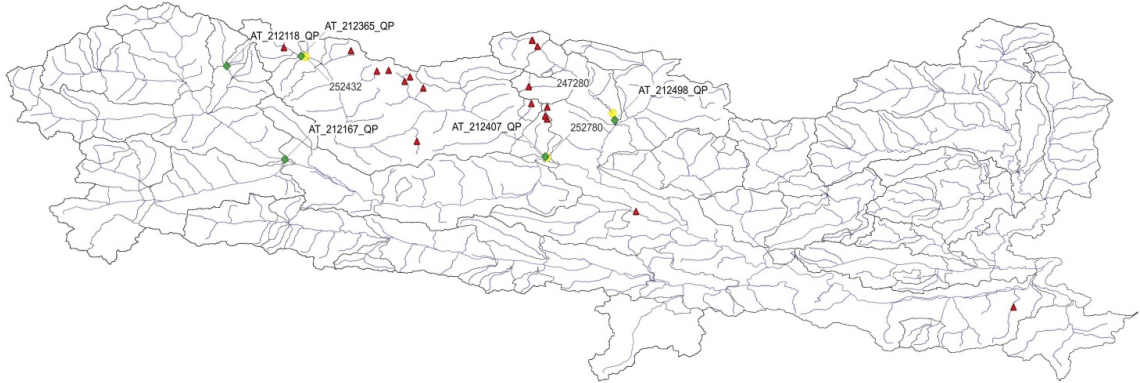


Figure 4.23: References for validation in the *Drau* catchment

4.4.1 GEV distribution

The data series available at the gauging stations cover both daily discharge values and annual maximum values: in the validation, the series of annual maximums were selected and a *Generalized Distribution of Extreme Values (GEV)* was fit to the data.

This type of function was developed in the context of *extreme value theory*, which allows statistical analysis of the probability of rare and extreme events: in our case, in fact, the return periods considered a part from 30 years, are 100 and 300 years. This function is defined by three real parameters referred to as μ , σ and ξ : these represent respectively the *location*, *scale* and *shape* of the distribution.

Fitting of the distribution to the real data was performed by applying the *fevd function* of the *exTremis package* available with the *R software*. Specifically, this function allows calculation by the *Maximum Likelihood Estimation* method of the discharge quantiles and their confidence intervals. The values obtained through this function will be used to calculate the percentage of peak reduction that will be compared with that obtained by applying the calculation routine.

Obviously, the uncertainty of this evaluation is closely related to the number of samples

analyzed: especially with very high return periods, such as those analyzed in our project, longer data series would be needed than those that are available in our case (Figure 4.24 and Figure 4.25).

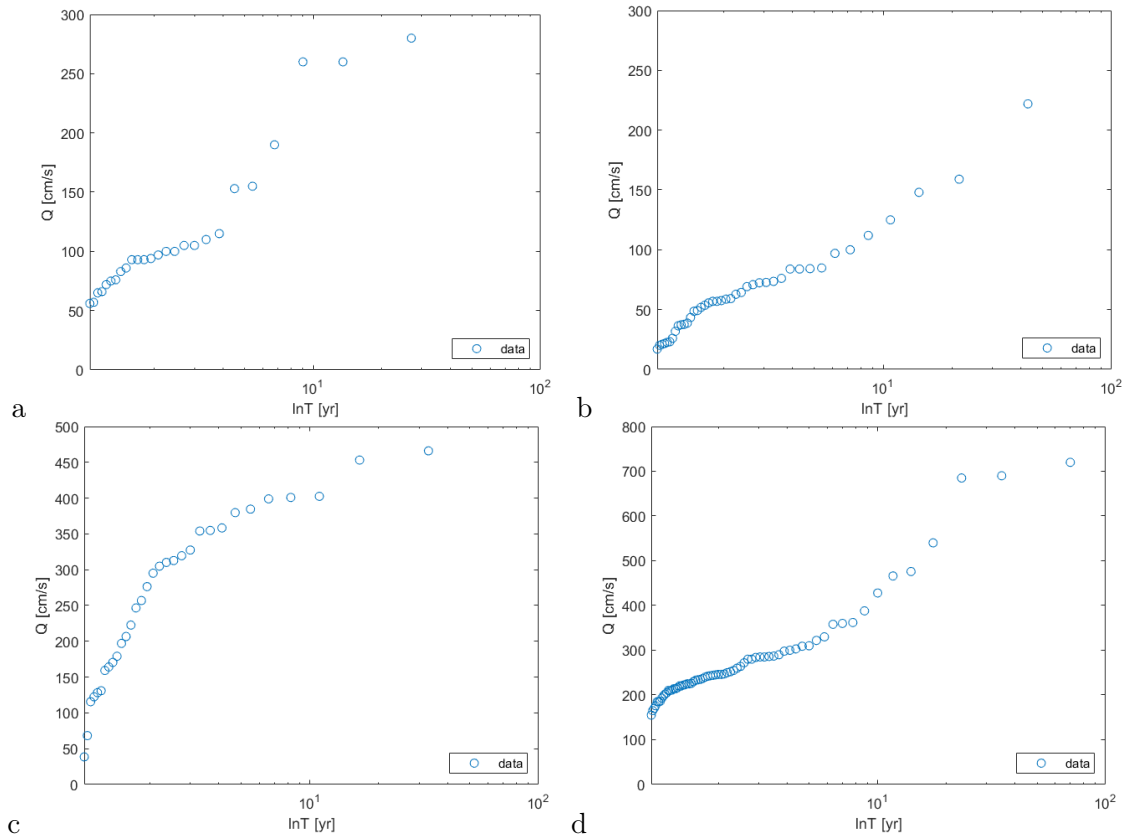


Figure 4.24: *Flood frequency curves for the validation stations in the Drau catchment (a: s212498 pre-dam period, b: s212498 post-dam period, c: s212407, d: s212167)*

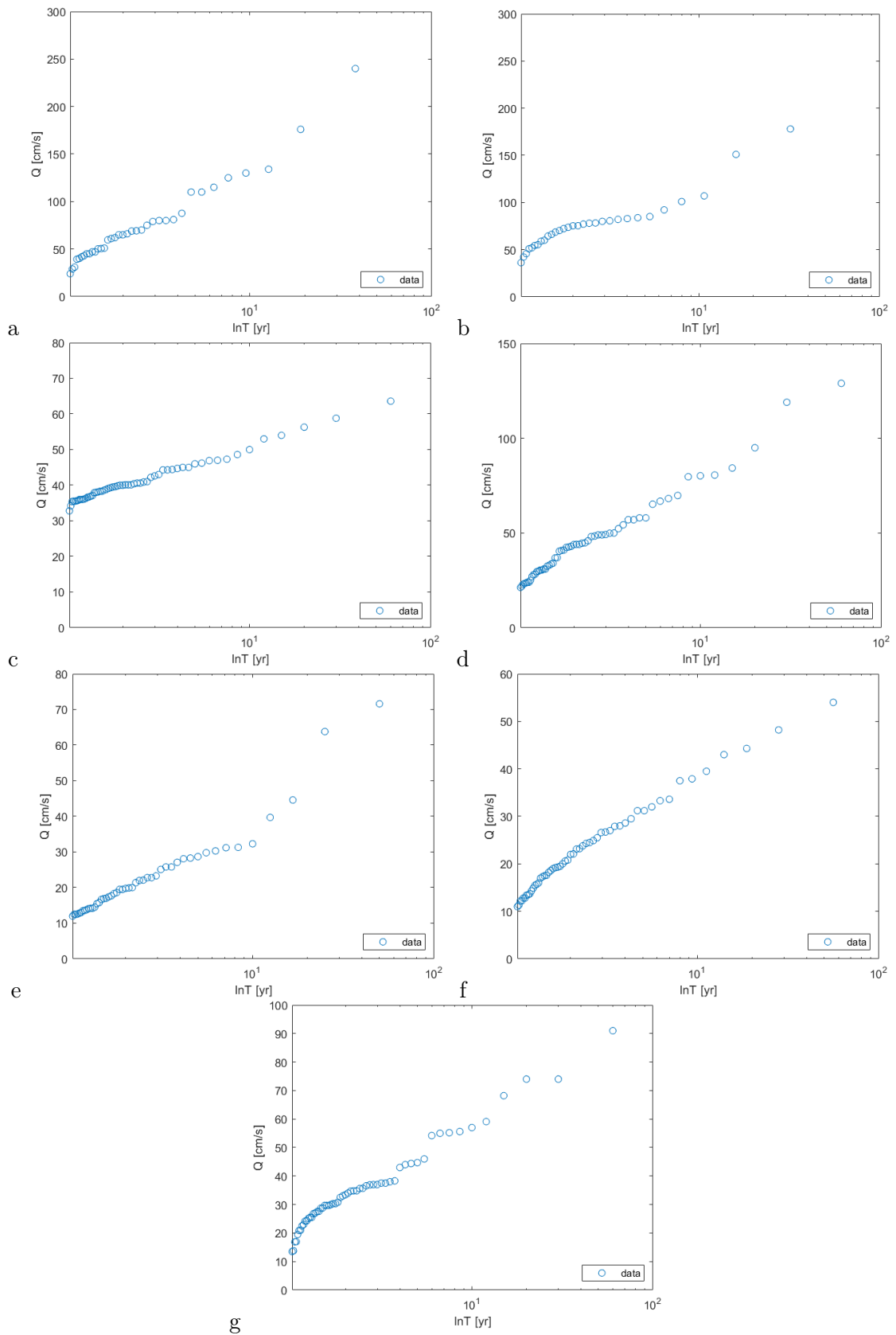


Figure 4.25: *Flood frequency curves* for the validation stations in the *Salzach catchment* (a: s203026 pre-dam period, b: s203026 post-dam period, c: s203109, d: s203034, e: s203042, f: s203083, g: s203158)

4.4.2 Validation in time

Validation in time is intended to compare the percentage of peak reduction derived using the model with the actual reduction that occurred due to the construction of one or more dams.

Specifically, the following steps were taken: (i) the gauging stations with the largest number of available data were selected for both basins, (ii) the data set was divided into two intervals representing the pre- and post-dam construction periods, (iii) two *GEV distributions* were fitted to these sub-series and from these the flow values for the return periods of 30, 100 and 300 years were derived (Figure 4.26).

Comparison was made between the percentage of peak reduction obtained at the calculation node closest to the selected measurement station and the percent value obtained at the station itself. The latter was obtained by applying the formula given in Table 4.6.

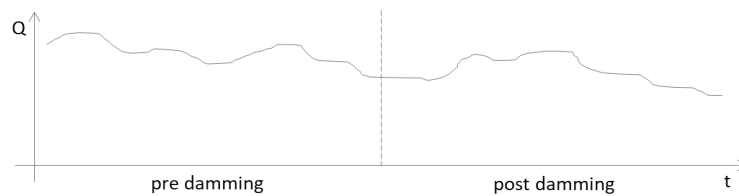


Figure 4.26: sketch on validation in time

$$\%R_{dataset} = \frac{HQ_{post-dam} - HQ_{pre-dam}}{HQ_{pre-dam}}$$

Table 4.6: Percentage of peak reduction from data set

For both the *Salzach* and *Drau catchments*, there is only enough data available at one gauging station to fit the *GEV distributions* in the two sub-intervals. For the *Salzach catchment*, at the selected gauging station annual maxima data are available for the period 1951-2019 and the dam considered during the validation was built in 1988. For the *Drau*

catchment, at the selected gauging station annual maxima data are available for the period 1951-2019 and the most recent of the dams considered during the validation was built in 1977.

4.4.3 Validation in space

Validation in space is intended to compare the percentage of peak reduction obtained using the model with the actual reduction that can be obtained by comparing discharges in two catchments, one of which is affected by the presence of one or more dams.

As analyzed by Merz and Blöschl (2005), catchments that are close to each other are characterized by similar flood response, as hydroclimatic and hydrogeological conditions are expected to change gradually over space.

Specifically, the following steps were taken: (i) catchments were chosen that were as close as possible and had characteristics in common (such as area, shape, topography, land cover and orientation), (ii) it was checked that sufficiently long data sets were available for the gauging stations located in the chosen basins and (iii) a *GEV distribution* was fitted to each set and from this the flow rate values for return periods of 30, 100, and 300 years were derived.

The comparison was made between the percentage of peak reduction obtained at the calculation node closest to the analyzed gauging station belonging to the basin affected by the presence of dams and the percent value obtained by comparing the two gauging stations chosen for validation (Figure 4.27). The latter is obtained by applying the formula given in Table 4.7.

In this case, validation was carried out by referring to the normalized discharge values obtained dividing the absolute discharge values, actually recorded at the gauging station,

with respect to the catchment area itself.

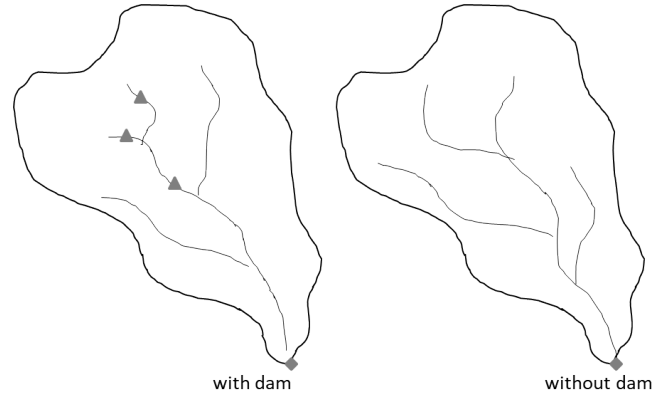


Figure 4.27: sketch on validation in space

$$\%R_{dataset} = \frac{Hq_{withdam} - Hq_{withoutdam}}{Hq_{withoutdam}}$$

$$Hq = \frac{HQ}{area_{catchment}} \quad [cm/skm]$$

Table 4.7: Percentage of peak reduction from data set

For the *Salzach catchment* two compatible basins have been found for the validation, while for the *Drau catchment* only one. The Table 4.8 provides the area of the upstream basin and the length of the data series for each gauging station considered during validation.

gauging station	area of the catchment upstream [skm]	duration of the series
203109	89.3	1961-2019
203034	81.1	1961-2019
203042	41.6	1971-2019
203083	74.3	1960-2019
203158	97.3	1960-2019
212407	1097.7	1984-2015
212167	1196.0	1951-2019

Table 4.8: Area of the upstream basin and the length of the data series for each gauging station considered during validation

4.4.4 Validation outcomes

For each of the points chosen for validation, as shown from Table 4.9 to Table 4.13, the percentage of peak reduction obtained by applying the calculation routine does not reflect exactly that obtained from the analysis of the discharge series at the gauging stations.

This means that, if the flood wave is large enough to be reduced and the volume of the dams is big enough to store all or part of the water from the flood event, our model produces a reduction that is smaller than the one derived from the data set.

gauging station	%R30 _{dataset}	%R100 _{dataset}	%R300 _{dataset}
203026	-0.224	-0.318	-0.392
computation node	%R30	%R100	%R300
239690	0.000	0.000	0.000

Table 4.9: Validation in time for the *Salzach* catchment

gauging station	%R30 _{dataset}	%R100 _{dataset}	%R300 _{dataset}
203109-203034	-0.490	-0.551	-0.591
203109-203042	-0.478	-0.578	-0.647
computation node	%R30	%R100	%R300
242060	-0.143	-0.162	-0.176

Table 4.10: Validation in space for the *Salzach* catchment

gauging station	%R30 _{dataset}	%R100 _{dataset}	%R300 _{dataset}
203083-203158	-0.147	-0.164	-0.181
computation node	%R30	%R100	%R300
194860	-0.014	-0.018	-0.020

Table 4.11: Validation in space for the *Salzach* catchment

gauging station	%R30 _{dataset}	%R100 _{dataset}	%R300 _{dataset}
212498	-0.409	-0.477	-0.545
computation node	%R30	%R100	%R300
247280	-0.112	-0.140	-0.157

Table 4.12: Validation in time for the *Drau catchment*

gauging station	%R30 _{dataset}	%R100 _{dataset}	%R300 _{dataset}
212407-212167	-0.067	-0.300	-0.482
computation node	%R30	%R100	%R300
252780	-0.036	-0.044	-0.035

Table 4.13: Validation in space for the *Drau catchment*

Using first the *ci* function of the *exTremis* package and then the *MOVERR* function of the *pairwiseCI* package, both of which can be implemented in the *R* software, it was possible to calculate the 95% confidence intervals of the discharge values for the return periods considered and associate them with each percentage of peak reduction. In this way, as can be seen in Figure 4.28 and Figure 4.29, it can be checked whether the results obtained from our model fall within these limits and thus what their reliability is.

The small number of data available at the analysed stations, even if they are those with more numerous series for both basins under analysis, implies that the percentage of reduction obtained is affected by a certain uncertainty and that the confidence intervals of these results are therefore wide.

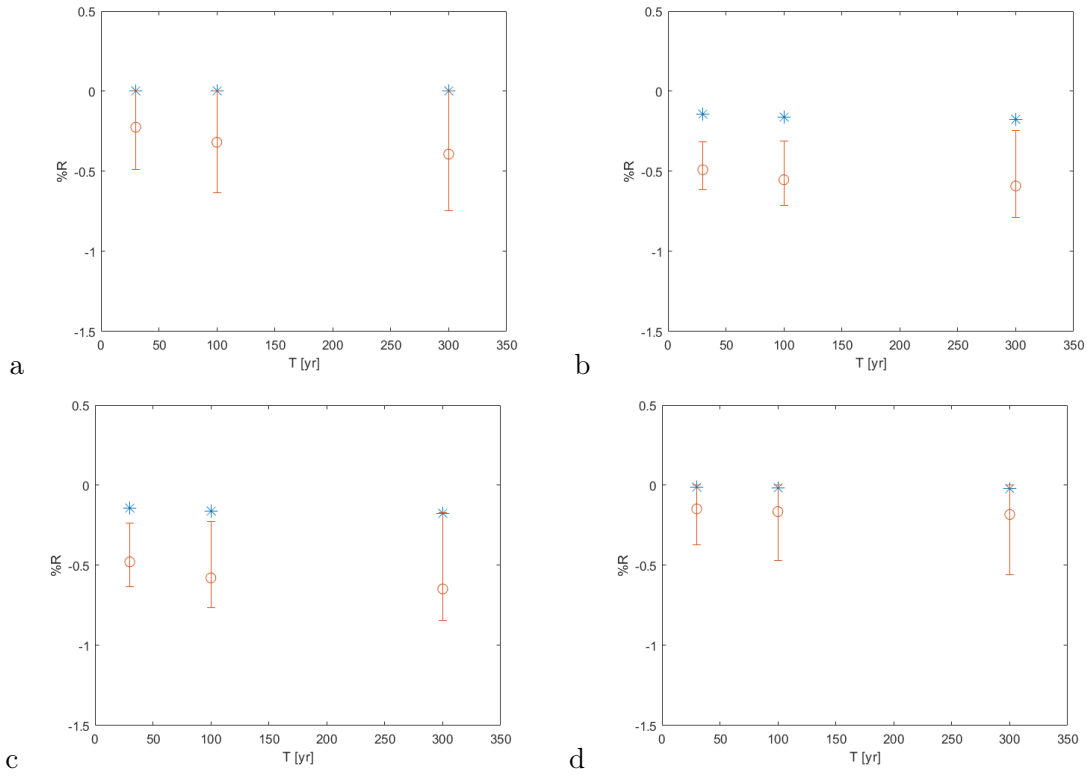


Figure 4.28: 95% confidence interval for the percentage of reduction of the peak in the *Salzach* catchment (a: s203026, b: s203109-s203034, c: s203109-s203042, d: s203083-s203158)

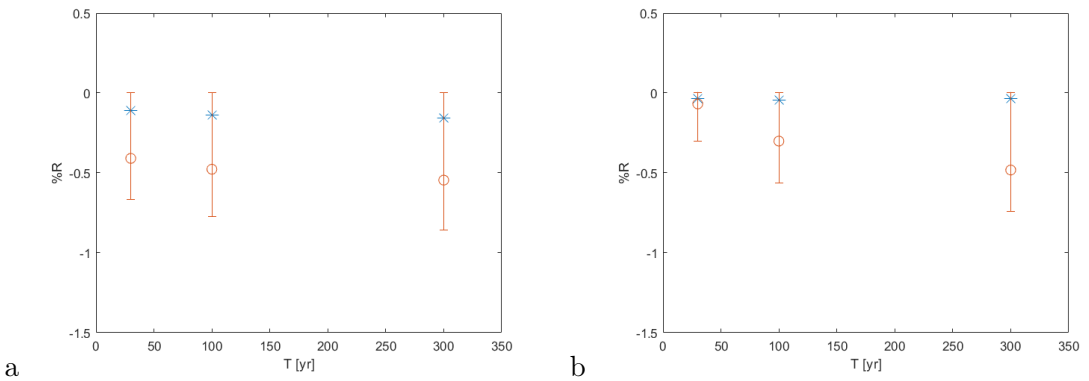


Figure 4.29: 95% confidence interval for the percentage of reduction of the peak in the *Drau* catchment (a: s212498, b: s212407-s212167)

4.5 Sensitivity analysis

In this last step, the aim is to analyse what changes could be applied to the model in order to improve its performance.

It was decided to act on three different elements: (i) the inlet hydrograph (ii) the *filling discharge* and (iii) the *protection ratio*.

4.5.1 Inlet hydrograph changes

As specified above in this method the input hydrograph for the peak reduction routine is defined by the way from the discharge values related to 30, 100 and 300 years. These values come from the *HORA 3.0 project* and therefore the data are obviously affected by the actual presence of the dams.

To improve the method, one could therefore derive flood curves with flow values referring to a period before the dams were built.

It should be noted that, regardless of what the results of this modification will be, it would be essential to improve the basic assumptions of the model: in this context, it was not applied at every computation node, but only for those used during the sensitivity analysis, for reasons of convenience and timing.

The changes in the inlet hydrograph can be done through two different ways, a temporal or spatial shift.

The first way consists in: (i) to derive the *GEV function* parameters by means of the MAF CV and CS values available from the *HORA 3.0 project* at each node; (ii) to draw in the *flood frequency plot* concerning the data series related to the period prior to the construction of the dams available at the respective stations and (iii) to translate the *CFR* obtained with the *GEV function* parameter according to the plot realized with the measurements at the stations.

The second way consists in identifying for each basin to which the nodes under analysis refer a similar one (in terms of area, shape, topography, land cover and orientation), but

characterised by the absence of dams. The flow values to describe the input hydrograph will be taken as those for this basin.

The first method, having a sufficiently long data set at the measuring station, was applied in the *Drau catchment* as shown in Table 4.15, while the second in the *Salzach catchment* as reported in Table 4.14.

The results show that the percentage of the peak reduction increases, as we expected, when considering the original curves: these in fact are characterised by higher values. However, the increase is not sufficient to reach the values, even if indicative, obtained from the data series at the measuring stations.

4.5.2 Filling discharge changes

This change consists, for each of the analysed nodes, in decreasing the *filling discharge* from the value obtained with the formula applied in the method.

The actual value of *filling discharge* obviously changes depending on the dam under analysis, and to know this, one would have to have the dam's management information available. For the purpose of this work, the formula from the *HORA 3.0 project* was applied, but it was defined specifically for *retention basins* and not for large dams, as in our case.

Table 4.14 and Table 4.15 show how the percentage of peak reduction changes as a function of the change in *filling discharge*.

Reducing the value of the *filling discharge* shows that the percentage of peak reduction increases, as there is still some volume available in the dams that allows more water to be stored. However, despite this change, the target values obtained from the data series are not reached. It should be noted that in some cases the value of the *filling discharge* is very low and, also if we don't know in detail the rules of dam utilisation, it may not make sense

to lower it further. In fact, one generally only starts storing water after a certain level, which is defined to act as conveniently as possible on the flood event.

4.5.3 Protection ratio changes

The last change made at this stage concerned the *protection ratio*, specifically for each of the analysed nodes this factor was increased from the value obtained in the method. In the previous case, the change was limited only to the directly modified parameter whereas now, by varying the *protection ratio*, the *filling discharge* will also be different as a consequence. As these dams are actually located very far upstream, the *protection ratio* decreases drastically at the downstream nodes, except for the first ones immediately after the dam, and this implies that a very small fraction of the total hydrograph can be acted upon.

Table 4.14 and Table 4.15 show how the percentage of peak reduction changes as a function of the change in *protection ratio*.

The results show that increasing the ratio significantly increases the percentage of peak reduction as the fraction of the curve on which the peak reduction routine is applied is bigger. In general, it can be seen that the best results, in terms of approaching the target values obtained from the data series, are achieved by acting on this coefficient.

	%R30 _{dataset}	%R100 _{dataset}	%R300 _{dataset}
gauging station			
203109-203034	-0.490	-0.551	-0.591
computation node	%R30	%R100	%R300
242060	-0.143	-0.162	-0.176
changing inlet hydrograph	%R30	%R100	%R300
	-0.159	-0.199	-0.225
changing Q _{filling}	%R30	%R100	%R300
8 cm/s	-0.203	-0.217	-0.226
6 cm/s	-0.239	-0.249	-0.256
4 cm/s	-0.275	-0.282	-0.287
changing PR	%R30	%R100	%R300
40%	-0.164	-0.187	-0.202
50%	-0.205	-0.233	-0.253
60%	-0.247	-0.280	-0.304
gauging station	%R30 _{dataset}	%R100 _{dataset}	%R300 _{dataset}
203083-203158	-0.147	-0.164	-0.181
computation node	%R30	%R100	%R300
194860	-0.014	-0.018	-0.020
changing inlet hydrograph	%R30	%R100	%R300
	-0.014	-0.018	-0.020
changing Q _{filling}	%R30	%R100	%R300
1 cm/s	-0.017	-0.019	-0.021
0.8 cm/s	-0.020	-0.022	-0.023
0.6 cm/s	-0.022	-0.024	-0.025
changing PR	%R30	%R100	%R300
10%	-0.046	-0.057	-0.063
20%	-0.093	-0.113	-0.127
30%	-0.139	-0.170	-0.190

Table 4.14: Sensitivity analysis for the *Salzach catchment*

	%R30 _{dataset}	%R100 _{dataset}	%R300 _{dataset}
gauging station			
212498	-0.409	-0.477	-0.545
computation node	%R30	%R100	%R300
247280	-0.112	-0.140	-0.157
changing inlet hydrograph	%R30	%R100	%R300
	-0.114	-0.140	-0.156
changing Q _{filling}	%R30	%R100	%R300
20 cm/s	-0.159	-0.177	-0.188
15 cm/s	-0.180	-0.193	-0.201
10 cm/s	-0.200	-0.209	-0.214
changing PR	%R30	%R100	%R300
30%	-0.139	-0.204	-0.212
40%	-0.186	-0.233	-0.261
50%	-0.232	-0.291	-0.326

Table 4.15: Sensitivity analysis for the *Drau catchments*

Chapter 5

Conclusions

This thesis work studied the combined effect on flood waves of large dams whose main purpose is power generation and that are located in nested catchments. The key point, as illustrated in this work, is to analyze how the reduction of the flood peak changes as one moves along the river network and as a function of different return periods. The approach consists of evaluating the design flood waves at different nodes in the river network and estimating the peak reduction for each point following the method applied in the *HORA 3.0 project*.

At the outset, simplifications related precipitation and flow values were assumed, and furthermore the discharge values treated, coming from the *HORA 3.0 project*, are to be considered as referring to the actual presence of the dams and thus generally lower than the conditions without these latter. During the application of the peak reduction routine, the transfer and allocation of the water resource and dam management techniques were not taken into account, the *filling discharge* was evaluated with the relationship found in the *HORA 3.0 project*, one unique *Gamma form* was considered in each computation node and finally the flood wave time parameter t_c was assumed constant for the different return periods analysed.

Our results show us that these dams, where sufficiently large, have a strong effect, albeit with no flood control measures, downstream. The effect is lost by moving far downstream for each of the return periods analyzed and for the different combinations of dams. The reduction is therefore generally felt in the basin to which the dam belongs, but after a confluence and in the context of the final section of a large basin such as the one of the *river Salzach* or of the *river Drau* it is negligible.

Surely there is potential to improve the method. For example, we did not change the value of t_c for different return periods and the *gamma function* for different locations along the river network: two aspects that affect the calculation of flood wave volume. Furthermore, in case of availability of the rules of dam use and thus of the actual available volume for flood control, the analysis could be detailed and improved according to the seasonality of floods. Finally, in order to avoid, where encountered, the problems of underestimation of the percentage of peak reduction, one could: working with flood waves prior to the construction of the dams, find a new formula for calculating the *filling discharge* that is specific to large dams and better define the application of the *protection ratio* in the splitting of the total hydrograph. The current use of the *protection ratio* is to multiply it by each hydrograph value so that the shape of the flood wave remains unchanged. In this way, the value of t_c is distorted as it is known that when a peak in a hydrograph is reduced, the volume is not reduced by the same amount and therefore the time parameter is higher than it actually is. Precisely the fact of having a higher t_c value implies a hydrograph that implies a larger volume and therefore the reduction that can be achieved, all other things being equal, is smaller.

Despite what has been said so far, this method can be considered a useful tool for calculating the reduction of flood wave peaks in ungauged basins, along the river network at

a regional scale. The framework, in fact, is easily generalizable and applicable in other contexts and precisely for this reason, it can be a functional tool to assess not only the percentage of reduction of a flood wave characterized by a specific return period, but also, from a spatial planning perspective, to define the downstream propagation of the effect of the dam so that preferential coordinates can be identified to make the best use of these structures also for flood control purposes.

Acknowledgements

Questo lavoro è il risultato di un'esperienza all'estero che è stata un'occasione straordinaria per portare a termine i miei studi. I mesi trascorsi a Vienna hanno contribuito ad arricchirmi sia tecnicamente che personalmente e sono sicura che ricorderò sempre questo periodo con particolare affetto.

Ora, concluso questo percorso, non resta che formulare i dovuti ringraziamenti.

Innanzitutto vorrei ringraziare il relatore di questa tesi, Prof. Alberto Viglione per avermi supervisionato e soprattutto fornito quest'ottima opportunità. Sono molto grata al correlatore, il Prof. Gunter Blöschl per i consigli che mi ha dato durante la mia permanenza all'interno del suo gruppo di ricerca senza i quali il mio progetto non avrebbe potuto prendere la giusta direzione. Un ringraziamento speciale è riservato alla Project Assistant Miriam Bertola, per il costante supporto che mi ha offerto: le occasioni di confronto avute insieme sono state sicuramente l'elemento chiave per la realizzazione di questo lavoro. Infine ringrazio il Senior Scientist Peter Valent, per avermi fornito le indicazioni e il materiale su cui si è basato fin dall'inizio il mio elaborato.

Non mi resta che rivolgermi a coloro che mi hanno accompagnato e sostenuto nella vita di tutti i giorni, in primis i miei genitori: è sicuramente grazie al loro supporto che sono riuscita ad arrivare alla fine dei miei studi. Un grazie sincero è riservato ad Alessio e a mia sorella Francesca, per tutti i consigli che hanno saputo darmi e per la fiducia che hanno

riposto in me sempre. Infine penso alle mie amiche storiche, ognuna a modo suo sa di essere stata la mia compagna di viaggio, e agli amici che ho avuto l'opportunità di incontrare durante questo percorso: non sapete quanto vi sono grata.

Bibliography

- [1] Bertola, M., Blöschl, G., Viglione, A. (2019), *Informed attribution of flood changes to decadal variation of atmospheric, catchment and river drivers in Upper Austria*. Journal of Hydrology, 577, 1-12
- [2] Cipollini, S., Fiori, A., & Volpi, E. (2022). *A new physically based index to quantify the impact of multiple reservoirs on flood frequency at the catchment scale based on the concept of equivalent reservoir*. Water Resources Research, 58, e2021WR031470.
<https://doi.org/10.1029/2021WR031470>
- [3] Blöschl, G., Waser, J., Buttinger-Kreuzhuber, A. et al. *HOchwasserRisikozonierung Austria 3.0 (HORA 3.0)*. Österr Wasser- und Abfallw 74, 212–223 (2022).
<https://doi.org/10.1007/s00506-022-00848-7>
- [4] Blöschl, Günter & Hall, Julia & Viglione, Alberto & Perdigao, Rui & Parajka, Juraj & Merz, Bruno & Lun, David & Arheimer, Berit & Aronica, G. & Bilibashi, Ardian & Boháč, Miloň & Bonacci, Ognjen & Borga, Marco & Čanjevac, Ivan & Castellarin, Attilio & Chirico, Giovanni Battista & Claps, Pierluigi & Frolova, N. & Ganora, Daniele & Nenad, Živković. (2019). *Changing climate both increases and decreases European river floods*. Nature. 573. 1-4. 10.1038/s41586-019-1495-6

- [5] Günter Blöschl et al. *Changing climate shifts timing of European floods*. *Science* 357, 588-590 (2017). DOI:10.1126/science.aan2506
- [6] G. Bloeschl, M. Sivapalan, T. Wagener, A. Viglione, & H. Savenije (Eds.), *Runoff Prediction in Ungauged Basins: Synthesis across Processes, Places and Scales* (pp. 163-188). Cambridge University Press
- [7] Donner A, Zou GY. *Closed-form confidence intervals for functions of the normal mean and standard deviation*. *Stat Methods Med Res*. 2012 Aug;21(4):347-59. doi: 10.1177/0962280210383082. Epub 2010 Sep 8. PMID: 20826501
- [8] Hall, J., Arheimer, B., Borga, M., Brázdil, R., Claps, P., Kiss, A., Kjeldsen, T. R., Kriaučiūnienė, J., Kundzewicz, Z. W., Lang, M., Llasat, M. C., Macdonald, N., McIntyre, N., Mediero, L., Merz, B., Merz, R., Molnar, P., Montanari, A., Neuhold, C., Parajka, J., Perdigão, R. A. P., Plavcová, L., Rogger, M., Salinas, J. L., Sauquet, E., Schär, C., Szolgay, J., Viglione, A., and Blöschl, G.: *Understanding flood regime changes in Europe: a state-of-the-art assessment*, *Hydrol. Earth Syst. Sci.*, 18, 2735–2772, <https://doi.org/10.5194/hess-18-2735-2014>, 2014
- [9] Lun, D., A. Viglione, M. Bertola, J. Komma, J. Parajka, P. Valent and G. Blöschl (2021), *Characteristics and process controls of statistical flood moments in Europe—a data based analysis*. *Hydrology and Earth System Sciences* 25, 5535-5560
- [10] Manfreda, S., Miglino, D., and Albertini, C.: *Impact of detention dams on the probability distribution of floods*, *Hydrol. Earth Syst. Sci.*, 25, 4231–4242, <https://doi.org/10.5194/hess-25-4231-2021>, 2021

- [11] Mei, Xuefei & Gelder, P.H.A.J.M. & Dai, Zhi-jun & Tang, Zhenghong. (2016). *Impact of dams on flood occurrence of selected rivers in the United States*. *Frontiers of Earth Science*. 11. 10.1007/s11707-016-0592-1
- [12] Merz, B., Vorogushyn, S., Uhlemann, S., Delgado, J., and Hundecha, Y.: *HESS Opinions "More efforts and scientific rigour are needed to attribute trends in flood time series"*, *Hydrol. Earth Syst. Sci.*, 16, 1379–1387, <https://doi.org/10.5194/hess-16-1379-2012>, 2012
- [13] Merz R., G. Blöschl and G. Humer (2008), *Hochwasserabflüsse in Österreich – das HORA-Projekt*. Österreichische Wasser- und Abfallwirtschaft, Heft 09-10/2008, S. 129-138
- [14] Merz R., G. Blöschl and G. Humer (2008), *National flood discharge mapping in Austria*. *Natural Hazards*, 46 (1), pp. 53-72
- [15] Merz, R., & Blöschl, G. (2005). *Flood Frequency Regionalisation - spatial proximity vs. catchment attributes*. *Journal of Hydrology*, 302(1–4), 283–306
- [16] Merz, R., G. Blöschl und U. Piöck-Ellena (1999), *Zur Anwendbarkeit des Gradex-Verfahrens in Österreich (Applicability of the Gradex-Method in Austria)*. Österreichische Wasser- und Abfallwirtschaft, 51, (11/12), pp. 291-305
- [17] Muhar, Susanne & Poppe, Michaela & Schmutz, Stefan & Jungwirth, Mathias. (2000). *Identification of rivers with high and good habitat quality: Methodological approach and applications in Austria*. *Hydrobiologia*. 422-423. 343-358. 10.1023/A:1017005914029
- [18] Schulz, K. *Alpine Hydrologie*. Österr Wasser und Abfallw 70, 460–461 (2018). <https://doi.org/10.1007/s00506-018-0525-1>

- [19] Gabriel Stecher & Mathew Herrnegger (2022) *Impact of hydropower reservoirs on floods: evidence from large river basins in Austria*, Hydrological Sciences Journal, 67:14, 2082-2099, DOI: 10.1080/02626667.2022.2130332
- [20] Volpi, E., Di Lazzaro, M., Bertola, M., Viglione, A., & Fiori, A. (2018). *Reservoir effects on flood peak discharge at the catchment scale*. Water resources Research, 54 <https://doi.org/10.1029/2018WR023866>
- [21] William L. Graf, *Downstream hydrologic and geomorphic effects of large dams on American rivers*, Geomorphology, Volume 79, Issues 3–4, 2006, Pages 336-360, ISSN 0169-555X, <https://doi.org/10.1016/j.geomorph.2006.06.022>
- [22] <https://www.icold-cigb.org>
- [23] <https://atcold.at>
- [24] <https://www.globaldamwatch.org/grand>
- [25] <https://www.hora.gv.at>

Annexes

Table 1: List of big dams in Austria

Dam ID	Latitude [°]	Longitude [°]	Capacity [Mcm]	Drainage area [skm]	Main type of use	Other uses
D_01_AT	47	13	4.30	2.34	hydroelectricity	-
D_02_AT	48	12	-	55.00	hydroelectricity	-
D_03_AT	47	13	14.20	5.00	hydroelectricity	flood control
D_04_AT	47	10	8.40	89.00	hydroelectricity	-
D_05_AT	48	13	4.80	11.92	hydroelectricity	-
D_06_AT	49	15	20.00	940.00	irrigation	-
D_07_AT	47	12	52.30	44.50	hydroelectricity	-
D_08_AT	47	13	0.15	38.90	hydroelectricity	-
D_09_AT	48	15	1.38	44.80	hydroelectricity	-
D_10_AT	47	13	1.20	1.60	hydroelectricity	-
D_11_AT	47	11	60.00	6.00	hydroelectricity	-
D_12_AT	47	14	5.30	44.40	hydroelectricity	-
D_13_AT	47	13	4.40	57.70	hydroelectricity	-
D_14_AT	47	11	138.30	107.30	hydroelectricity	-
D_15_AT	47	12	0.74	144.00	hydroelectricity	-
D_16_AT	47	13	0.06	9.40	hydroelectricity	-
D_17_AT	48	14	25.00	34.00	hydroelectricity	-
D_18_AT	47	13	1.80	10.80	hydroelectricity	-
D_19_AT	47	13	7.72	2.51	hydroelectricity	-
D_20_AT	47	13	9.20	1.70	hydroelectricity	-
D_21_AT	47	15	7.60	160.00	hydroelectricity	-
D_22_AT	47	13	4.11	1.52	hydroelectricity	-
D_23_AT	47	13	7.60	5.60	hydroelectricity	-
D_24_AT	47	12	0.17	67.00	hydroelectricity	-
D_25_AT	48	14	13.35	539.00	hydroelectricity	flood control
D_26_AT	47	13	2.77	1.43	hydroelectricity	-
D_27_AT	47	10	44.00	7.30	hydroelectricity	-
D_28_AT	47	11	3.00	23.00	hydroelectricity	-
D_29_AT	47	15	0.32	170.00	hydroelectricity	-
D_30_AT	47	13	83.00	36.30	hydroelectricity	-
D_31_AT	47	10	78.30	9.30	hydroelectricity	-
D_32_AT	47	10	0.07	180.00	hydroelectricity	-
D_33_AT	47	13	3.20	44.40	hydroelectricity	-
D_34_AT	47	13	85.40	21.80	hydroelectricity	-
D_35_AT	47	13	0.06	37.40	hydroelectricity	-
D_36_AT	47	13	33.00	1.70	hydroelectricity	-
D_37_AT	49	15	51.20	889.00	hydroelectricity	flood control

D_38_AT	47	14	0.22	107.00	hydroelectricity	-
D_39_AT	47	15	5.60	63.00	hydroelectricity	-
D_40_AT	47	13	2.54	1.68	hydroelectricity	-
D_41_AT	47	10	2.00	160.00	hydroelectricity	-
D_42_AT	49	14	2.30	164.00	hydroelectricity	-
D_43_AT	47	13	15.60	9.87	hydroelectricity	-
D_44_AT	47	11	1.10	62.00	hydroelectricity	-
D_45_AT	48	14	10.67	150.00	hydroelectricity	-
D_46_AT	47	13	1.10	0.51	hydroelectricity	-
D_47_AT	47	12	127.40	58.20	hydroelectricity	-
D_48_AT	47	10	38.60	34.60	hydroelectricity	-
D_49_AT	47	15	16.20	29.80	hydroelectricity	-
D_50_AT	47	14	1.50	141.00	hydroelectricity	-
D_51_AT	47	10	15.70	11.10	hydroelectricity	-
D_52_AT	47	10	15.70	11.10	hydroelectricity	-
D_53_AT	47	12	6.45	61.40	hydroelectricity	-
D_54_AT	48	13	2.50	100.00	hydroelectricity	-
D_55_AT	47	13	55.30	22.40	Hydroelectricity	flood control
D_56_AT	49	15	0.80	1015.00	hydroelectricity	-
D_57_AT	47	10	5.00	56.60	hydroelectricity	-
D_58_AT	47	10	0.29	52.60	-	-
D_59_AT	47	13	15.70	5.42	hydroelectricity	-
D_60_AT	47	14	1.15	153.40	hydroelectricity	-
D_61_AT	48	15	0.16	31.70	hydroelectricity	-
D_62_AT	48	16	-	-	-	-
D_63_AT	48	13	7.50	175.00	hydroelectricity	-
D_64_AT	47	13	2.70	21.10	hydroelectricity	-
D_65_AT	47	12	86.70	30.00	hydroelectricity	-
D_66_AT	47	13	8.65	2.70	hydroelectricity	-
D_67_AT	47	12	-	67.80	-	-
D_68_AT	47	13	205.00	51.30	hydroelectricity	-
D_69_AT	49	16	-	32.50	-	-
D_70_AT	47	11	1.70	2.25	hydroelectricity	-
D_71_AT	47	12	-	18.10	-	-
D_72_AT	47	13	0.22	67.10	hydroelectricity	-
D_73_AT	47	13	85.40	21.80	hydroelectricity	-
D_74_AT	47	12	0.06	110.00	-	-
D_75_AT	47	13	3.20	44.40	hydroelectricity	-
D_76_AT	47	13	190.00	51.30	hydroelectricity	-
D_77_AT	47	10	0.03	98.00	hydroelectricity	-
D_78_AT	47	13	0.08	22.16	hydroelectricity	-

Figure 1: Salzach catchment

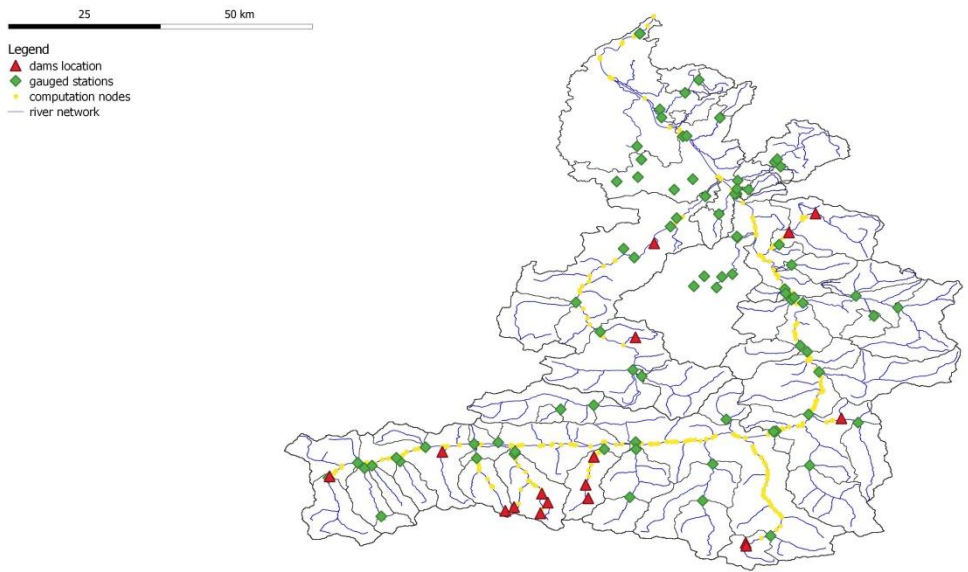


Figure 2: Drau catchment

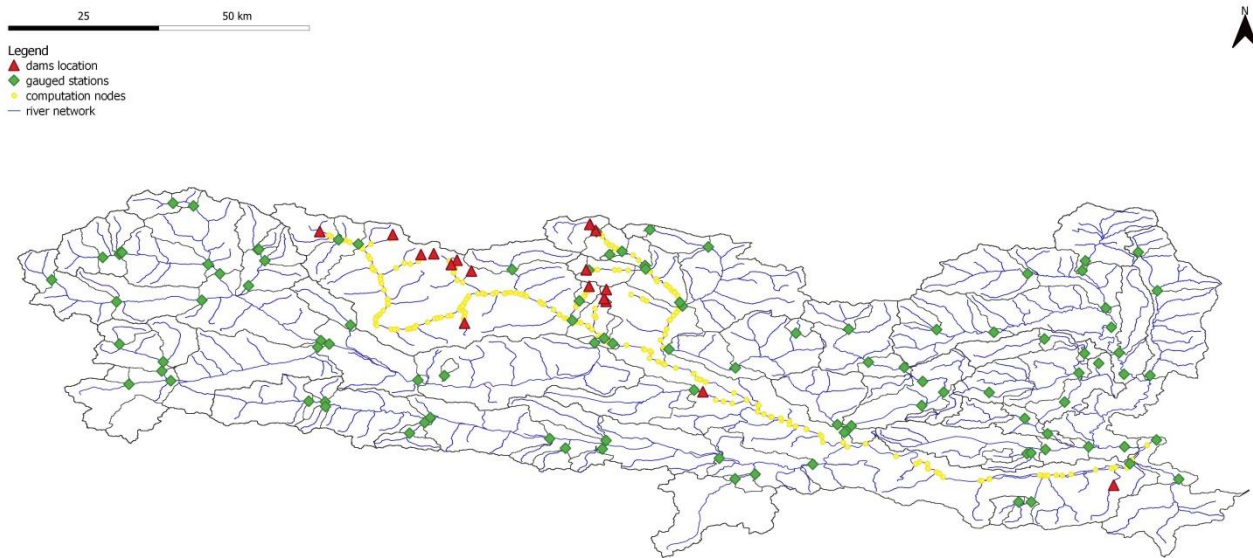


Figure 3: Available values for the time constant

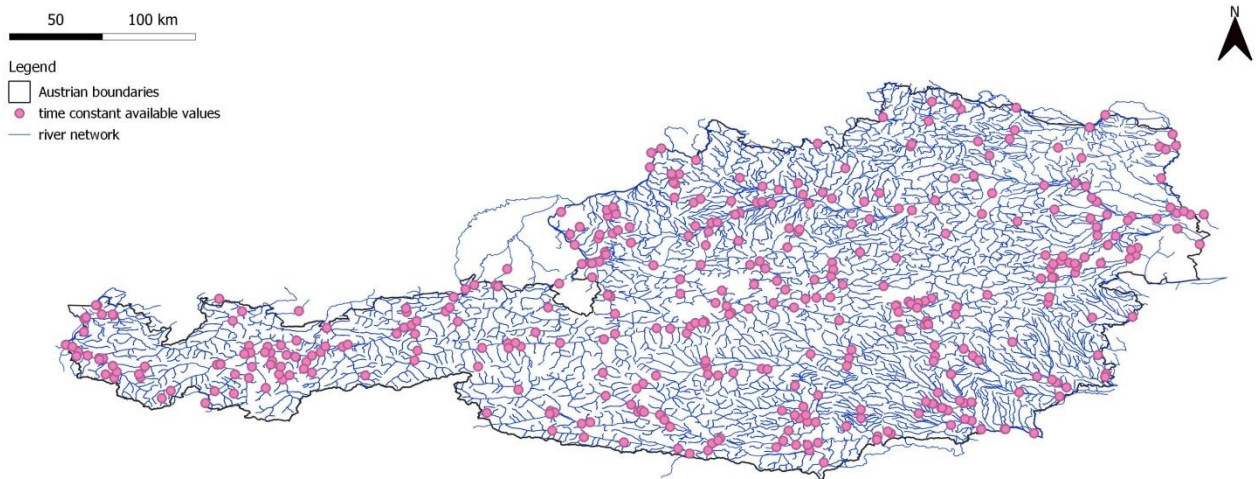


Figure 4: Area upstream nodes

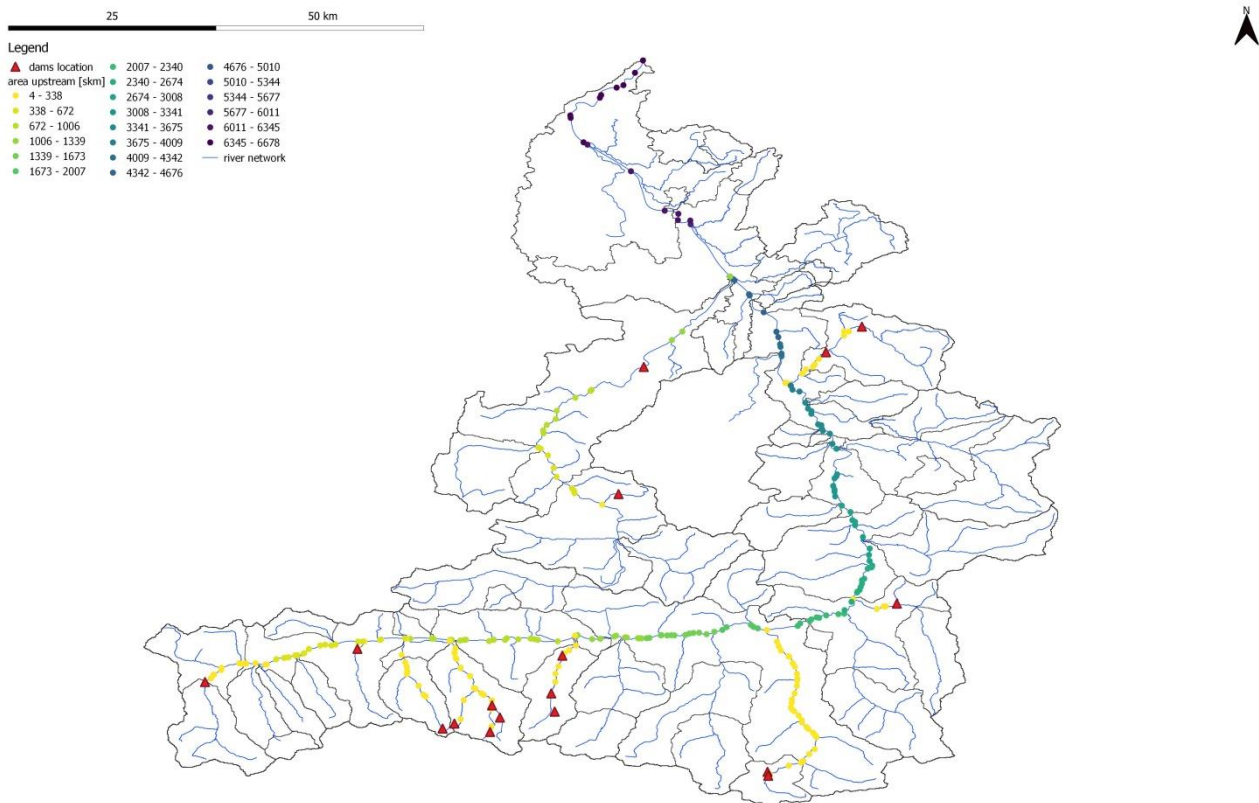


Figure 5: Flood event duration

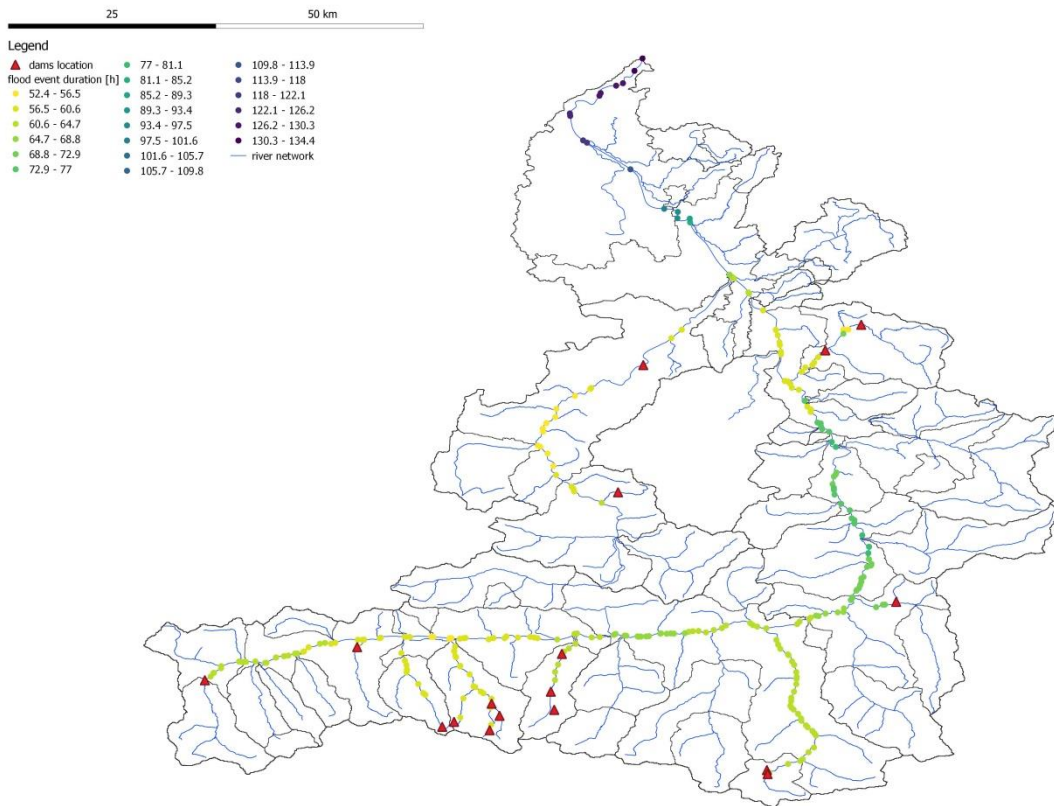


Figure 6: Protection ratio

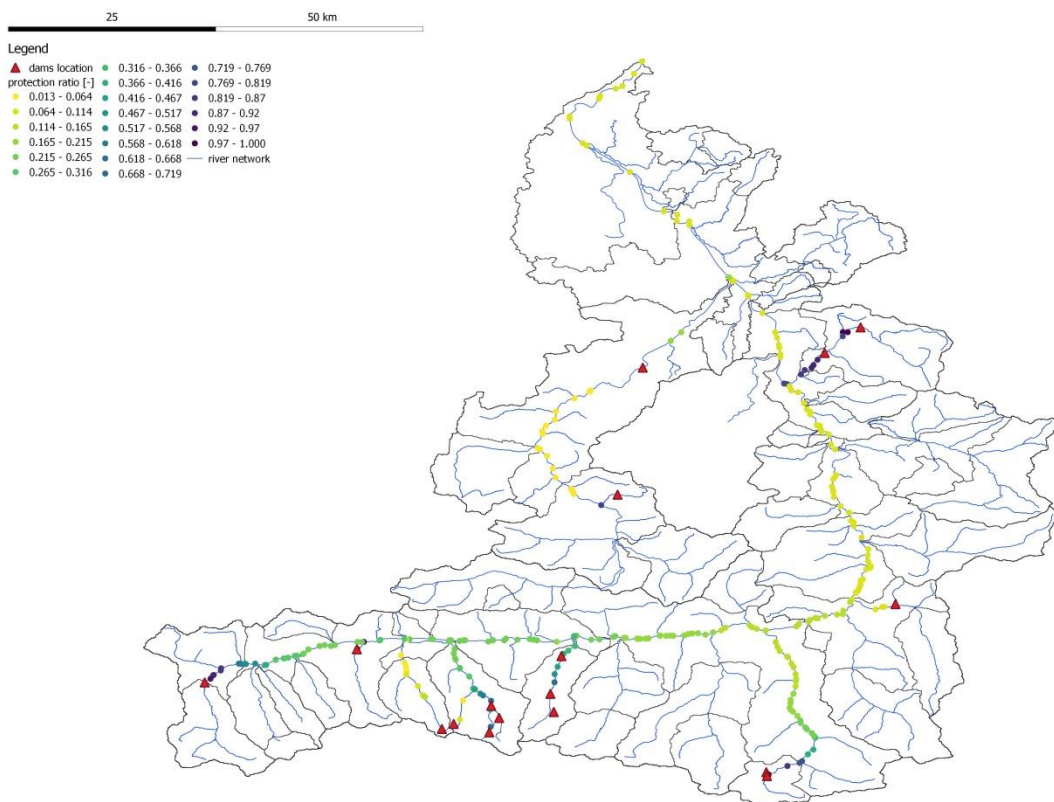


Figure 7: Mean annual discharge

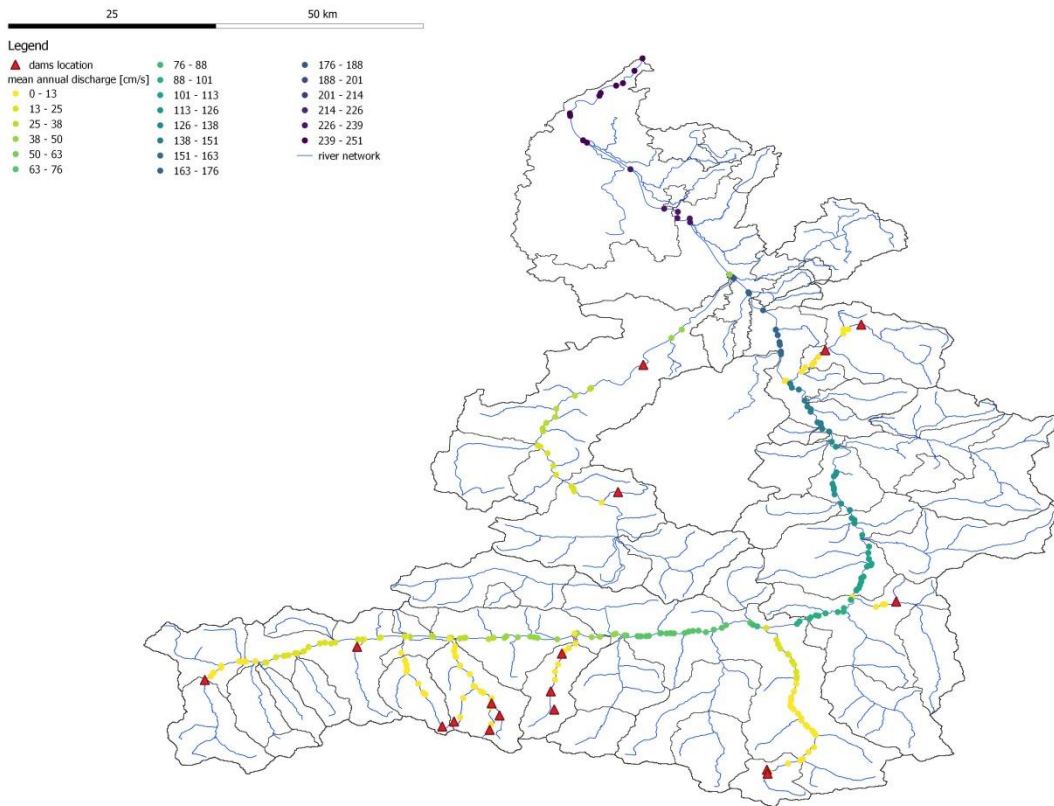


Figure 8: Peak discharge for 30 years

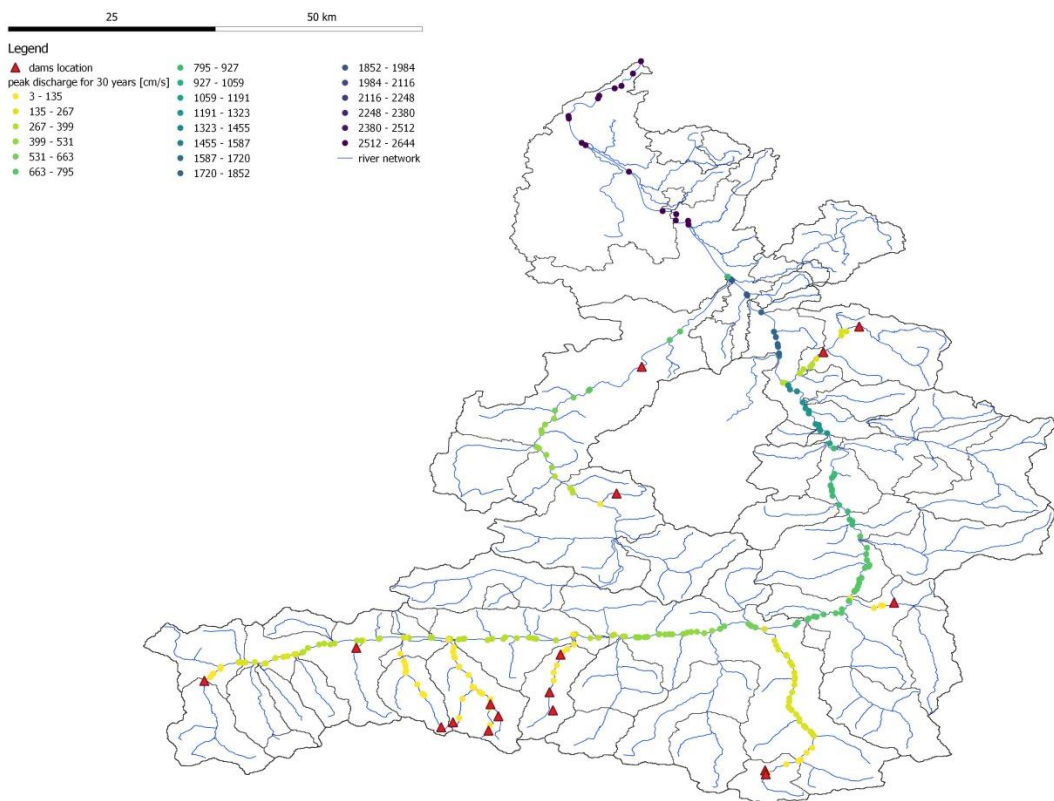


Figure 9: Peak discharge for 100 years

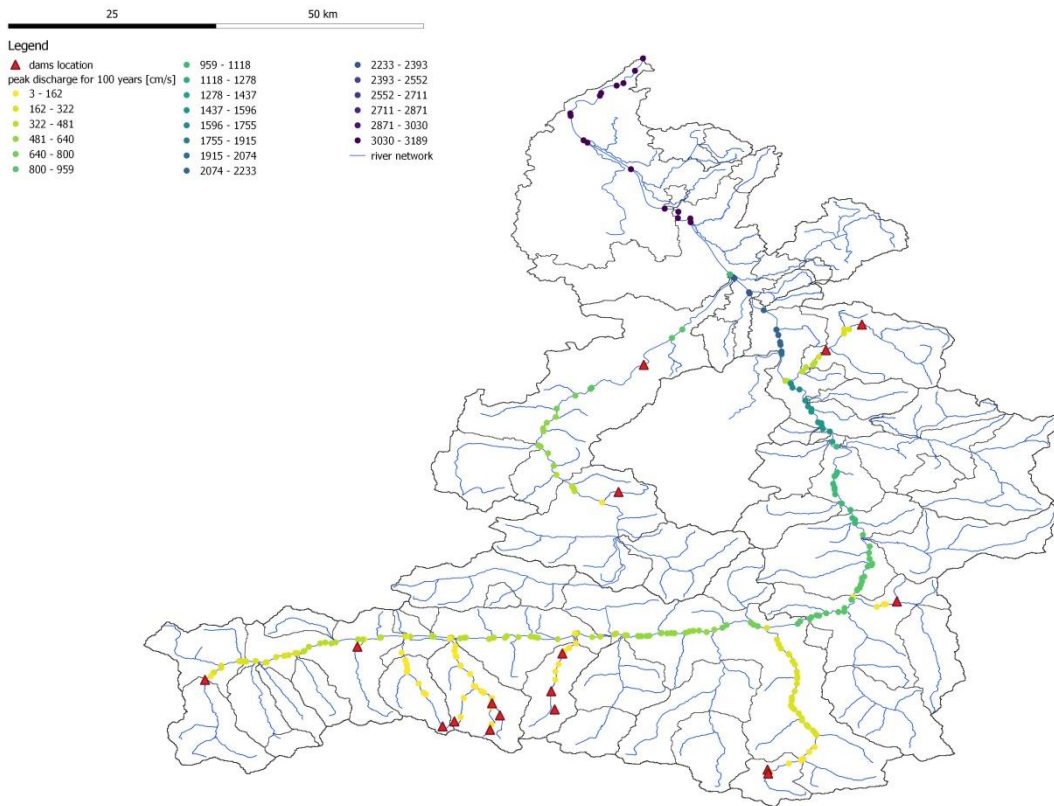


Figure 10: Peak discharge for 300 years

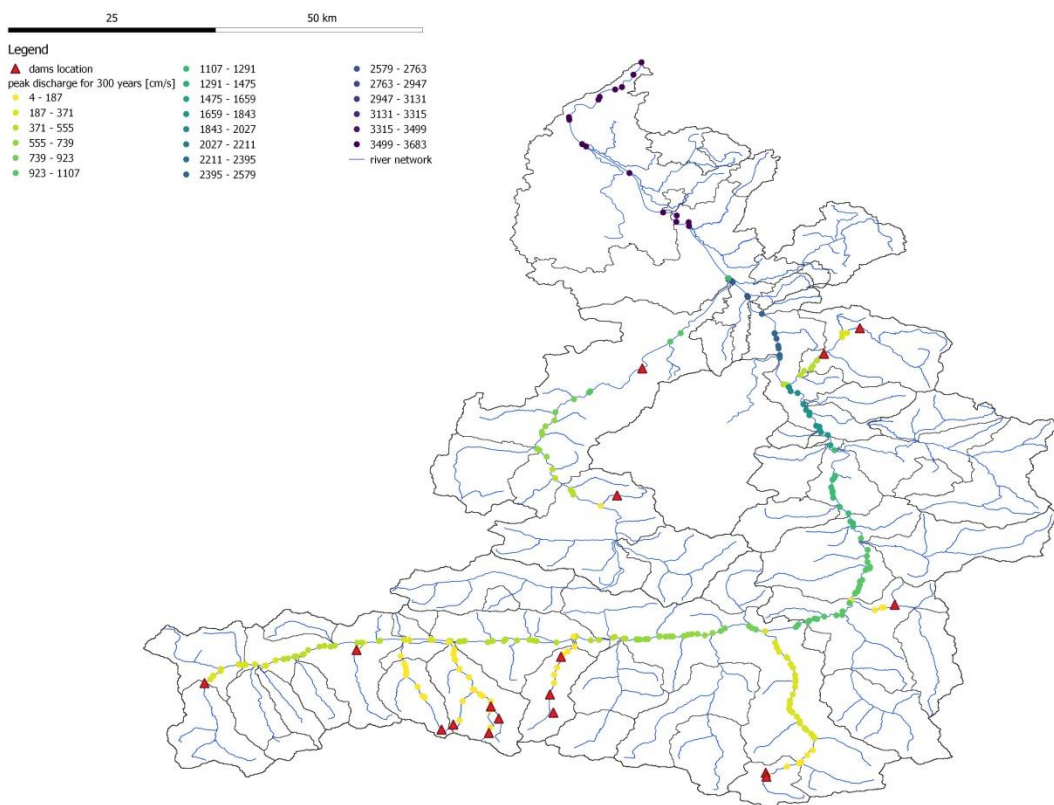


Figure 11: Filling discharge

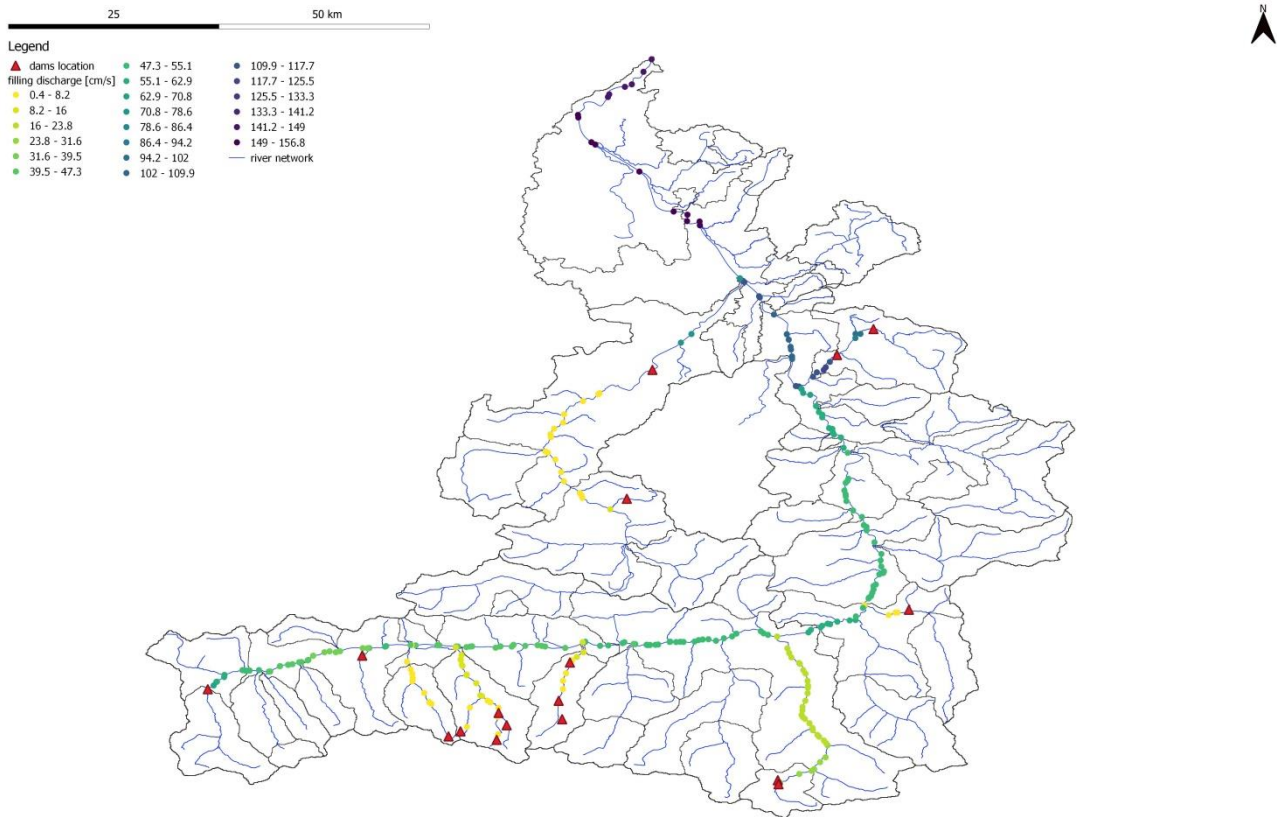


Figure 12: Area upstream nodes

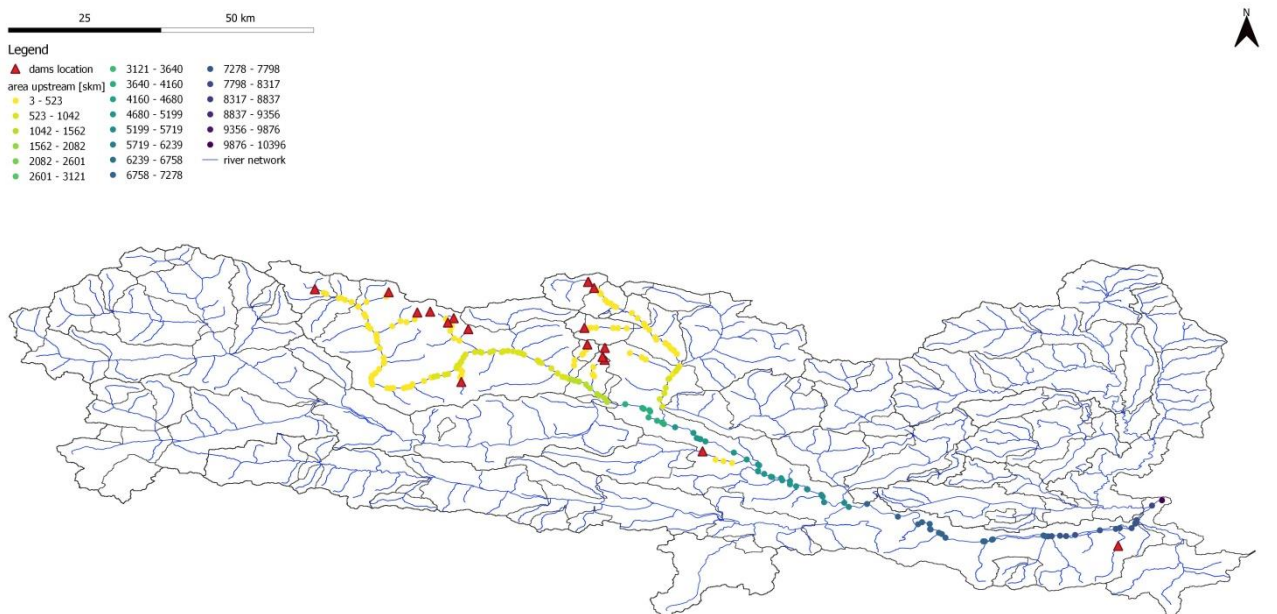


Figure 13: Flood event duration

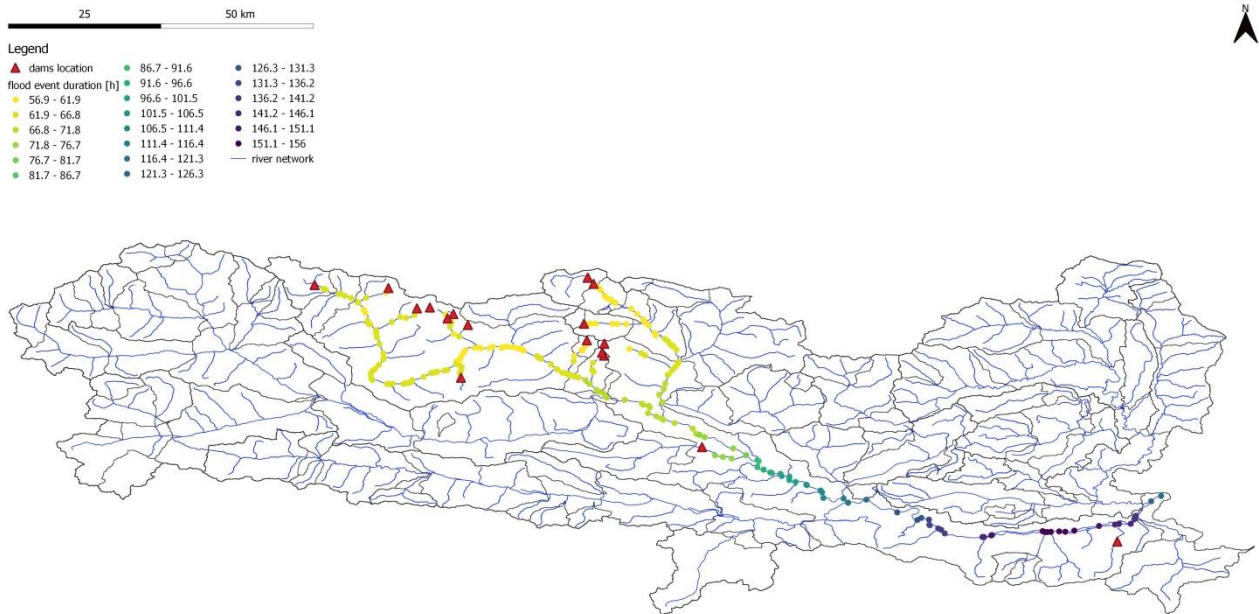


Figure 14: Protection ratio

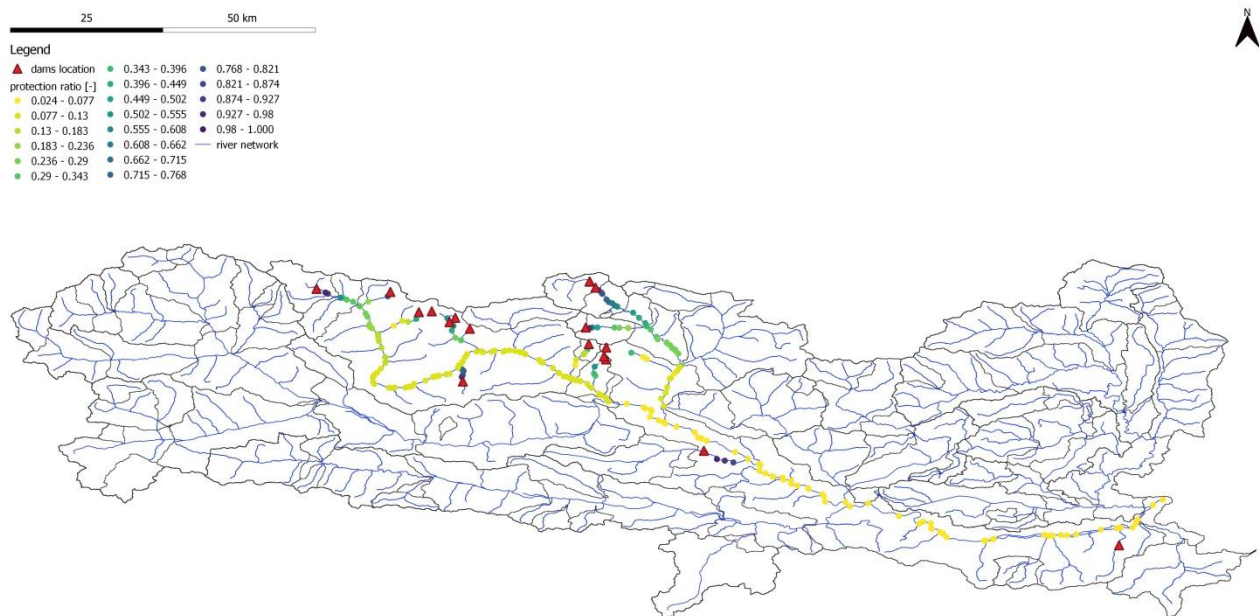


Figure 15: Mean annual discharge

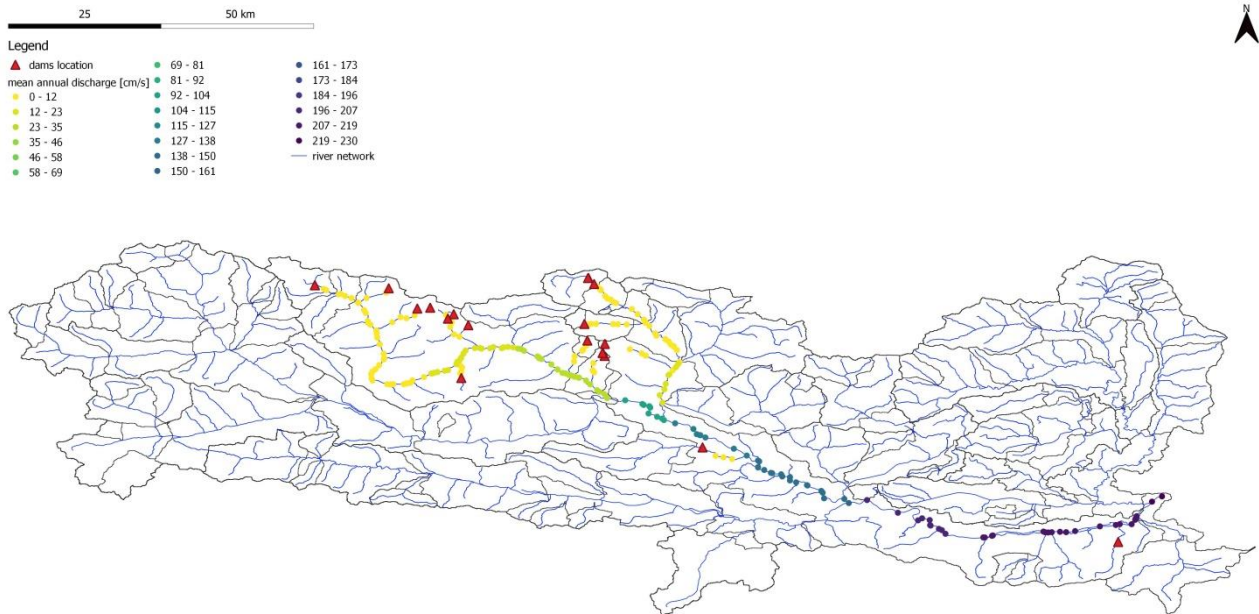


Figure 16: Peak discharge for 30 years

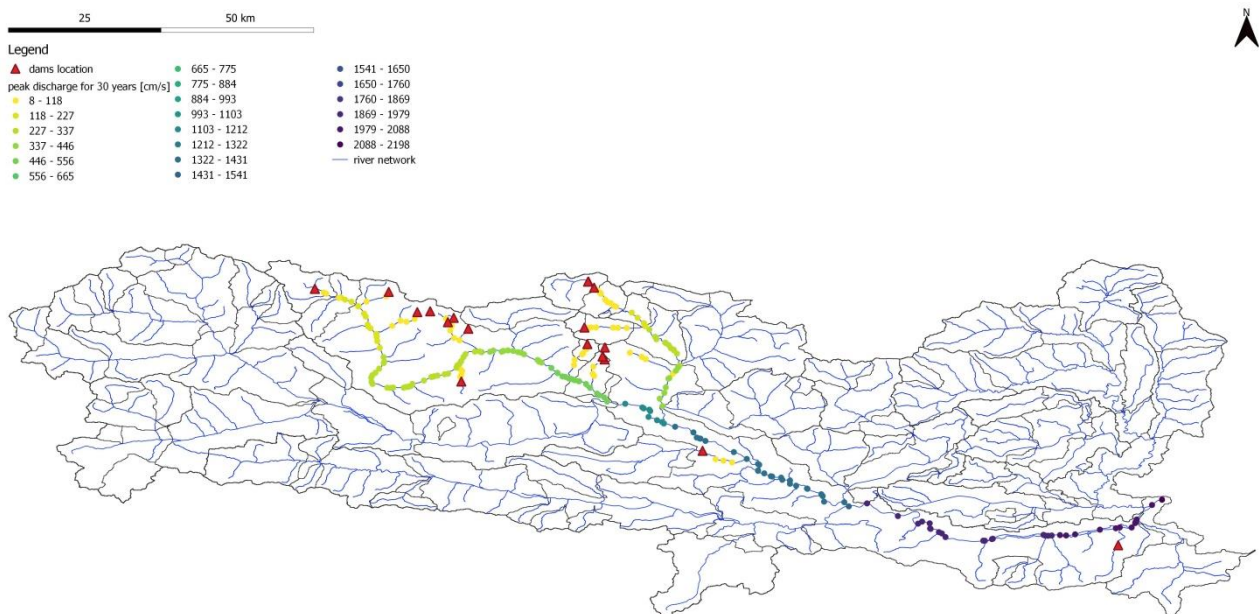


Figure 17: Peak discharge for 100 years

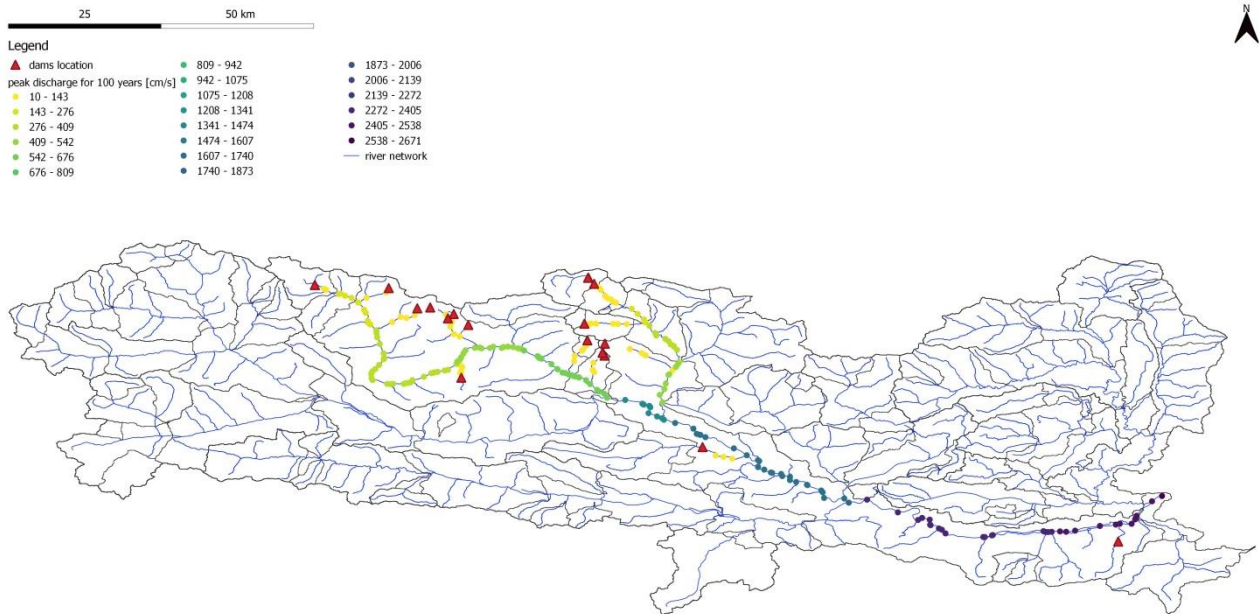


Figure 18: Peak discharge for 300 years

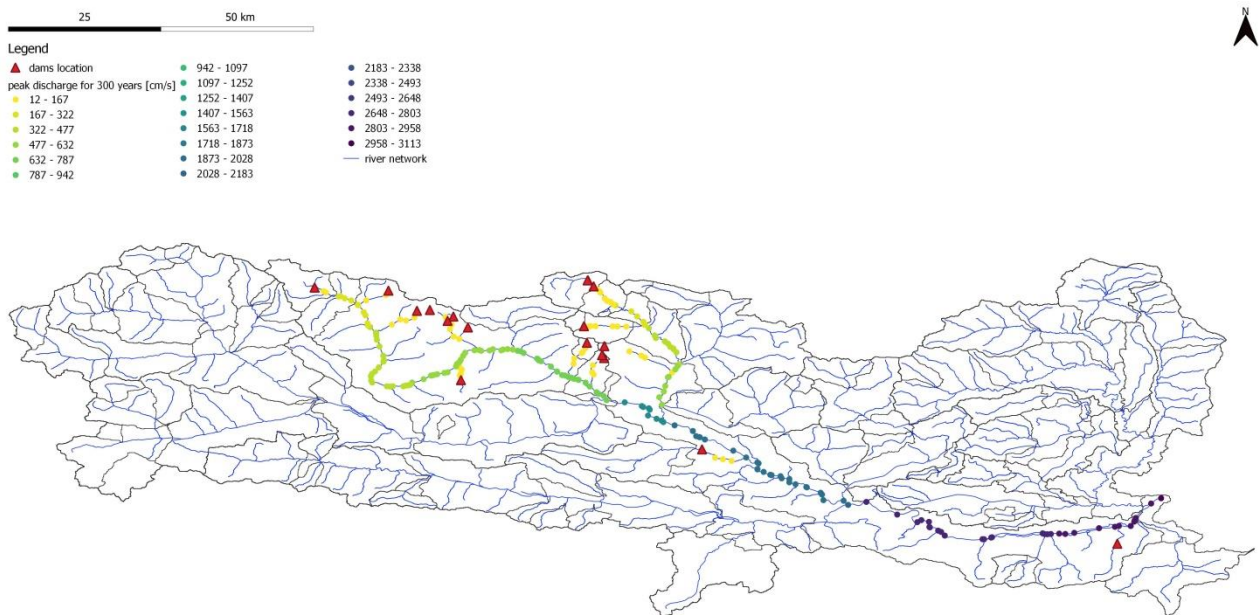


Figure 19: Filling discharge

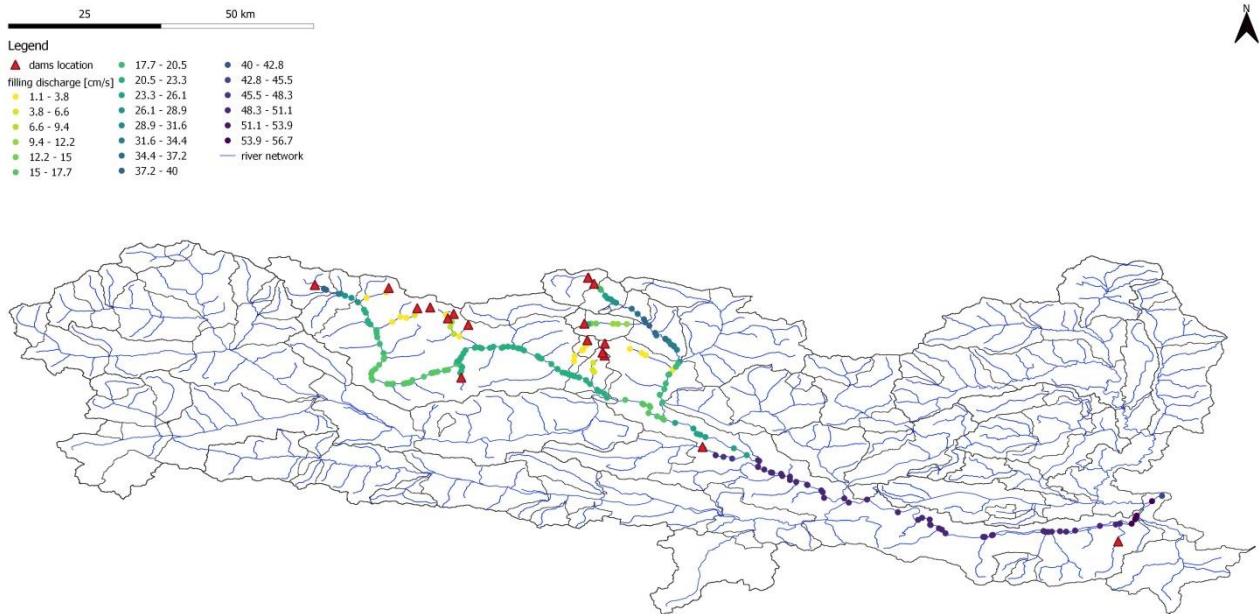


Table 2: Percentage of peak reduction in the Salzach catchment

Computation node	%R30	%R100	%R300
100501	-0.032	-0.039	-0.044
100502	-0.265	-0.142	-0.086
103310	-0.267	-0.143	-0.086
103362	-0.032	-0.040	-0.045
103412	-0.067	-0.036	-0.025
103471	0.000	-0.087	-0.201
103472	-0.103	-0.160	-0.197
103512	-0.161	-0.054	-0.017
103521	0.000	0.000	0.000
105471	0.000	0.000	0.000
194570	-0.279	-0.138	-0.076
194580	-0.282	-0.139	-0.076
194590	-0.259	-0.124	-0.095
194601	-0.266	-0.130	-0.101
194610	0.000	0.000	0.000
194620	-0.282	-0.138	-0.076
194631	-0.005	0.000	0.000
194640	-0.004	0.000	0.000
194680	-0.005	0.000	0.000
194850	-0.017	-0.021	-0.023
194860	-0.014	-0.018	-0.020
194870	-0.016	-0.019	-0.022
194910	-0.017	-0.020	-0.023
194930	-0.018	-0.022	-0.024

194942	-0.033	-0.041	-0.045
196850	-0.014	-0.017	-0.019
196860	-0.057	-0.069	-0.076
197990	-0.323	-0.392	-0.436
198010	-0.040	-0.049	-0.055
198020	-0.050	-0.060	-0.067
198030	-0.058	-0.071	-0.079
198050	-0.059	-0.072	-0.080
199150	0.000	0.000	0.000
199511	0.000	0.000	0.000
199530	0.000	0.000	0.000
199550	0.000	0.000	0.000
199600	0.000	0.000	0.000
199820	0.000	0.000	0.000
199830	0.000	0.000	0.000
199890	0.000	0.000	0.000
199910	0.000	0.000	0.000
199950	0.000	0.000	0.000
200950	0.000	0.000	0.000
200960	-0.160	-0.053	-0.016
200970	-0.154	-0.064	-0.020
201050	0.000	0.000	0.000
237431	-0.397	-0.472	-0.520
237450	-0.006	-0.008	-0.009
237462	-0.007	-0.008	-0.009
237502	-0.010	-0.011	-0.012
237512	-0.058	-0.029	-0.017
237520	-0.059	-0.030	-0.018
237602	-0.007	-0.009	-0.010
237621	-0.007	-0.008	-0.009
237631	-0.007	-0.008	-0.009
237640	-0.009	-0.011	-0.012
237651	-0.009	-0.011	-0.012
237660	-0.009	-0.011	-0.012
237672	-0.011	-0.012	-0.014
237682	-0.010	-0.012	-0.013
237810	-0.007	-0.009	-0.010
237920	-0.007	-0.009	-0.009
237930	-0.011	-0.012	-0.014
237940	-0.006	-0.008	-0.008
237950	-0.011	-0.013	-0.014
237970	-0.047	-0.063	-0.072
237981	-0.050	-0.065	-0.075
237990	-0.038	-0.050	-0.057
238000	-0.038	-0.050	-0.057
238011	-0.039	-0.051	-0.058
238020	0.000	0.000	0.000

238031	0.000	0.000	0.000
238041	-0.034	-0.044	-0.050
238052	-0.032	-0.040	-0.046
238062	0.000	0.000	0.000
238070	-0.057	-0.076	-0.088
238080	-0.079	-0.101	-0.116
238091	0.000	0.000	0.000
238101	0.000	0.000	0.000
238102	-0.133	-0.151	-0.164
238110	-0.058	-0.077	-0.089
238120	0.000	0.000	0.000
238130	0.000	0.000	0.000
238140	0.000	0.000	0.000
238150	0.000	0.000	0.000
238160	-0.038	-0.050	-0.057
238171	-0.035	-0.046	-0.053
238181	-0.038	-0.049	-0.056
238190	-0.032	-0.039	-0.044
238200	-0.032	-0.039	-0.044
238211	0.000	0.000	0.000
238212	-0.013	-0.016	-0.018
238220	0.000	0.000	0.000
238230	-0.047	-0.063	-0.072
238240	-0.041	-0.054	-0.062
238250	-0.032	-0.040	-0.045
238260	-0.032	-0.040	-0.045
238280	-0.048	-0.063	-0.072
238290	-0.038	-0.049	-0.056
238310	-0.040	-0.052	-0.059
238320	0.000	0.000	0.000
238331	-0.047	-0.063	-0.072
238352	0.000	0.000	0.000
238360	-0.058	-0.077	-0.090
238370	-0.077	-0.099	-0.114
238380	-0.078	-0.100	-0.114
238390	-0.059	-0.078	-0.091
238400	0.000	0.000	0.000
238410	-0.039	-0.051	-0.059
238420	-0.040	-0.051	-0.059
238430	-0.039	-0.051	-0.059
238440	0.000	0.000	0.000
238450	0.000	0.000	0.000
238460	0.000	0.000	0.000
238471	0.000	0.000	0.000
238480	0.000	0.000	0.000
238490	0.000	0.000	0.000
238500	0.000	0.000	0.000

238511	-0.046	-0.061	-0.070
238520	-0.041	-0.054	-0.062
238531	-0.040	-0.047	-0.033
238540	-0.039	-0.051	-0.058
238550	0.000	0.000	0.000
238561	-0.035	-0.046	-0.052
238570	-0.034	-0.045	-0.052
238600	-0.058	-0.077	-0.090
238610	-0.058	-0.077	-0.090
238621	0.000	0.000	0.000
238630	0.000	0.000	0.000
238640	0.000	0.000	0.000
238652	0.000	0.000	0.000
238660	0.000	0.000	0.000
238670	-0.046	-0.061	-0.070
238680	-0.047	-0.063	-0.072
238690	-0.034	-0.045	-0.051
238700	-0.048	-0.063	-0.073
238710	-0.040	-0.052	-0.059
238720	-0.040	-0.052	-0.059
238731	-0.041	-0.054	-0.062
238732	0.000	0.000	0.000
238740	-0.048	-0.064	-0.073
238750	-0.041	-0.051	-0.038
238762	-0.032	-0.040	-0.045
238770	-0.032	-0.040	-0.045
238780	-0.032	-0.040	-0.045
238790	-0.034	-0.045	-0.051
238800	0.000	0.000	0.000
238810	0.000	0.000	0.000
238820	0.000	0.000	0.000
238830	0.000	0.000	0.000
238842	0.000	0.000	0.000
238851	-0.034	-0.044	-0.050
238860	0.000	0.000	0.000
238871	-0.077	-0.099	-0.114
238881	-0.071	-0.092	-0.106
238890	-0.058	-0.078	-0.090
238900	-0.043	-0.052	-0.040
238911	-0.038	-0.050	-0.057
238920	-0.047	-0.058	-0.051
238930	-0.077	-0.099	-0.114
238970	-0.057	-0.075	-0.088
238980	-0.057	-0.075	-0.088
238990	-0.056	-0.074	-0.086
239000	0.000	0.000	0.000
239011	-0.048	-0.062	-0.072

239012	-0.052	-0.038	-0.028
239020	-0.048	-0.063	-0.073
239030	-0.048	-0.062	-0.073
239041	-0.034	-0.045	-0.051
239050	-0.056	-0.074	-0.086
239060	-0.056	-0.074	-0.086
239070	-0.058	-0.077	-0.090
239082	-0.032	-0.040	-0.045
239090	-0.034	-0.044	-0.050
239100	-0.034	-0.044	-0.050
239110	-0.034	-0.044	-0.050
239120	-0.056	-0.074	-0.086
239130	-0.040	-0.049	-0.037
239140	0.000	0.000	0.000
239150	0.000	0.000	0.000
239160	0.000	0.000	0.000
239170	-0.040	-0.052	-0.059
239180	0.000	0.000	0.000
239191	-0.057	-0.075	-0.088
239201	-0.057	-0.076	-0.089
239211	0.000	0.000	0.000
239221	0.000	0.000	0.000
239230	0.000	0.000	0.000
239242	-0.041	-0.044	-0.030
239252	-0.040	-0.046	-0.033
239260	-0.040	-0.050	-0.037
239270	-0.032	-0.040	-0.045
239282	-0.046	-0.057	-0.051
239290	-0.041	-0.054	-0.062
239300	-0.032	-0.040	-0.045
239312	-0.040	-0.050	-0.040
239320	-0.034	-0.044	-0.050
239330	-0.039	-0.046	-0.032
239340	-0.042	-0.052	-0.040
239350	-0.034	-0.044	-0.050
239361	-0.051	-0.066	-0.076
239372	-0.056	-0.073	-0.086
239380	0.000	0.000	0.000
239390	-0.028	-0.016	-0.005
239401	-0.040	-0.046	-0.036
239402	-0.051	-0.030	-0.017
239410	-0.032	-0.039	-0.044
239420	-0.032	-0.039	-0.044
239430	-0.035	-0.014	-0.008
239441	-0.039	-0.019	-0.007
239451	-0.029	-0.017	-0.005
239461	-0.032	-0.013	-0.008

239471	-0.045	-0.020	-0.010
239480	-0.043	-0.016	-0.012
239490	-0.040	-0.017	-0.010
239500	-0.032	-0.017	-0.010
239510	-0.042	-0.017	-0.007
239520	-0.033	-0.013	-0.008
239530	-0.035	-0.015	-0.009
239540	-0.038	-0.018	-0.006
239550	-0.043	-0.020	-0.009
239560	-0.043	-0.020	-0.009
239570	0.000	0.000	0.000
239582	0.000	0.000	0.000
239590	0.000	0.000	0.000
239600	0.000	0.000	0.000
239612	0.000	0.000	0.000
239620	0.000	0.000	0.000
239630	-0.051	-0.066	-0.076
239640	-0.057	-0.076	-0.088
239650	-0.043	-0.052	-0.040
239660	-0.034	-0.044	-0.050
239670	-0.038	-0.016	-0.009
239680	0.000	0.000	0.000
239690	0.000	0.000	0.000
241480	-0.140	-0.207	-0.249
241490	-0.095	-0.120	-0.135
241502	-0.089	-0.112	-0.126
241511	-0.011	-0.013	-0.015
241512	-0.178	-0.225	-0.254
241520	-0.133	-0.210	-0.259
241530	-0.090	-0.113	-0.128
241540	-0.094	-0.119	-0.134
241550	0.000	-0.120	-0.200
241572	-0.112	-0.142	-0.161
241580	-0.115	-0.146	-0.165
241590	-0.135	-0.170	-0.192
241600	-0.124	-0.157	-0.177
241610	-0.098	-0.123	-0.139
241620	-0.098	-0.123	-0.139
241660	-0.084	-0.037	-0.023
241670	-0.057	-0.042	-0.026
241680	-0.051	-0.028	-0.015
241690	-0.057	-0.041	-0.024
241700	-0.071	-0.041	-0.020
241710	-0.078	-0.038	-0.023
241720	-0.076	-0.040	-0.019
241730	-0.073	-0.039	-0.019
241740	-0.065	-0.042	-0.024

241750	-0.101	-0.039	-0.016
241760	-0.100	-0.039	-0.016
241772	-0.088	-0.036	-0.016
241780	-0.056	-0.042	-0.026
241790	-0.067	-0.038	-0.026
241800	-0.065	-0.043	-0.024
241810	-0.059	-0.038	-0.027
241820	-0.067	-0.037	-0.012
241830	-0.056	-0.042	-0.026
241840	-0.069	-0.032	-0.019
241850	-0.069	-0.038	-0.025
241860	-0.060	-0.026	-0.012
241872	-0.065	-0.030	-0.015
241880	-0.068	-0.033	-0.018
241890	-0.079	-0.039	-0.013
241900	-0.068	-0.039	-0.014
241910	-0.070	-0.038	-0.020
242060	-0.143	-0.162	-0.176
242070	-0.091	-0.133	-0.162
242080	-0.109	-0.143	-0.168
242090	0.000	0.000	-0.019
242100	-0.114	-0.140	-0.159
242110	0.000	0.000	-0.017
242120	-0.148	-0.168	-0.182
242130	0.000	0.000	0.000
270790	-0.182	-0.230	-0.260

Table 3: Percentage of peak reduction in the Drau catchment

Computation node	%R30	%R100	%R300
105522	-0.091	-0.114	-0.128
105602	-0.301	-0.108	-0.047
105830	-0.010	-0.013	-0.014
105882	-0.040	-0.049	-0.036
105892	-0.061	-0.080	-0.057
105902	-0.049	-0.063	-0.052
105911	-0.036	-0.044	-0.035
105942	-0.006	-0.001	0.000
242540	-0.411	-0.518	-0.580
242600	-0.080	-0.100	-0.112
242610	-0.213	-0.267	-0.298
243550	-0.025	-0.205	-0.308
243672	-0.006	-0.001	0.000
245062	-0.006	-0.001	0.000
247170	-0.242	-0.301	-0.336

247180	-0.341	-0.440	-0.498
247190	-0.341	-0.439	-0.498
247201	-0.152	-0.190	-0.213
247211	-0.087	-0.095	-0.062
247212	-0.184	-0.229	-0.256
247220	-0.298	-0.375	-0.421
247230	-0.321	-0.408	-0.460
247240	-0.219	-0.272	-0.303
247250	-0.292	-0.367	-0.412
247261	-0.280	-0.350	-0.392
247270	-0.196	-0.241	-0.269
247280	-0.112	-0.140	-0.157
247290	-0.190	-0.233	-0.260
247300	-0.117	-0.146	-0.164
247310	-0.115	-0.145	-0.163
247320	-0.115	-0.144	-0.161
247332	-0.139	-0.173	-0.194
247340	-0.351	-0.463	-0.530
247350	-0.131	-0.163	-0.183
247360	-0.122	-0.153	-0.171
247370	-0.120	-0.151	-0.169
247380	-0.123	-0.154	-0.173
247480	0.000	0.000	0.000
247490	0.000	0.000	0.000
247510	0.000	0.000	0.000
247520	0.000	0.000	0.000
247810	-0.202	-0.253	-0.284
247820	-0.529	-0.663	-0.741
247830	-0.162	-0.204	-0.229
247840	-0.283	-0.353	-0.395
247850	-0.240	-0.301	-0.338
247860	-0.095	-0.119	-0.133
247871	-0.135	-0.169	-0.190
247880	-0.253	-0.318	-0.357
248021	-0.044	-0.056	-0.063
248022	-0.018	-0.022	-0.024
248030	-0.044	-0.056	-0.063
248040	-0.041	-0.053	-0.060
248111	-0.108	-0.135	-0.151
248190	-0.042	-0.053	-0.060
248200	-0.045	-0.057	-0.064
248210	-0.041	-0.052	-0.059
248222	-0.041	-0.052	-0.058
248232	-0.039	-0.049	-0.055
248320	-0.039	-0.049	-0.056
248562	-0.006	-0.001	0.000
249080	-0.044	-0.054	-0.060

249090	-0.186	-0.227	-0.252
249100	-0.088	-0.106	-0.118
249110	-0.039	-0.047	-0.052
249120	-0.067	-0.081	-0.090
250311	-0.023	-0.023	-0.023
251452	-0.004	-0.002	0.000
251660	-0.150	-0.180	-0.199
251670	-0.198	-0.239	-0.265
251680	-0.271	-0.328	-0.362
251720	-0.039	-0.046	-0.051
251730	-0.177	-0.215	-0.239
251740	-0.028	-0.033	-0.037
252002	-0.017	-0.017	-0.017
252020	-0.100	-0.102	-0.061
252030	-0.051	-0.067	-0.054
252040	-0.051	-0.067	-0.053
252050	-0.034	-0.047	-0.031
252060	-0.007	-0.007	-0.006
252070	-0.050	-0.065	-0.052
252080	-0.045	-0.060	-0.044
252090	-0.045	-0.060	-0.043
252100	-0.153	-0.080	-0.039
252110	-0.119	-0.102	-0.058
252122	-0.177	-0.076	-0.031
252130	-0.142	-0.088	-0.048
252140	-0.322	-0.117	-0.027
252161	-0.113	-0.136	-0.151
252162	-0.036	-0.045	-0.029
252172	-0.052	-0.067	-0.046
252180	-0.049	-0.030	-0.018
252190	-0.048	-0.036	-0.022
252200	-0.050	-0.065	-0.045
252210	-0.049	-0.064	-0.044
252220	-0.051	-0.065	-0.045
252230	-0.053	-0.068	-0.042
252240	-0.054	-0.070	-0.043
252252	-0.042	-0.054	-0.038
252260	-0.041	-0.053	-0.037
252270	-0.042	-0.055	-0.038
252280	-0.051	-0.065	-0.053
252290	-0.050	-0.065	-0.053
252300	-0.050	-0.064	-0.052
252310	-0.052	-0.039	-0.020
252320	-0.051	-0.039	-0.020
252332	-0.051	-0.057	-0.038
252341	-0.020	-0.026	-0.029
252342	-0.082	-0.092	-0.051

252350	-0.083	-0.093	-0.050
252361	-0.030	-0.036	-0.040
252362	-0.009	-0.008	-0.008
252370	-0.043	-0.052	-0.049
252380	-0.035	-0.045	-0.029
252390	-0.055	-0.056	-0.054
252400	-0.036	-0.046	-0.036
252410	-0.036	-0.044	-0.036
252420	-0.034	-0.045	-0.037
252432	-0.253	-0.095	-0.031
252440	-0.070	-0.091	-0.058
252450	-0.107	-0.098	-0.056
252462	-0.097	-0.099	-0.059
252470	-0.005	-0.005	-0.004
252480	-0.005	-0.005	-0.004
252490	-0.005	-0.005	-0.004
252501	-0.133	-0.081	-0.043
252502	-0.040	-0.051	-0.057
252510	-0.035	-0.046	-0.029
252520	-0.034	-0.045	-0.037
252530	-0.061	-0.068	-0.054
252540	-0.055	-0.073	-0.048
252550	-0.050	-0.066	-0.053
252561	0.000	0.000	0.000
252562	-0.010	-0.009	-0.009
252570	-0.047	-0.052	-0.049
252580	-0.055	-0.057	-0.055
252590	-0.007	-0.007	-0.007
252601	-0.038	-0.047	-0.034
252610	-0.038	-0.046	-0.037
252620	-0.038	-0.049	-0.033
252630	-0.050	-0.038	-0.019
252640	-0.038	-0.050	-0.034
252650	-0.038	-0.050	-0.034
252660	-0.038	-0.050	-0.034
252670	-0.054	-0.035	-0.021
252680	-0.052	-0.040	-0.020
252690	-0.034	-0.045	-0.037
252702	-0.067	-0.093	-0.063
252712	-0.056	-0.073	-0.059
252720	-0.078	-0.101	-0.061
252730	-0.072	-0.094	-0.060
252750	-0.044	-0.059	-0.043
252762	-0.007	-0.007	-0.007
252770	-0.038	-0.046	-0.037
252780	-0.036	-0.044	-0.035
252791	-0.088	-0.110	-0.123

252792	-0.051	-0.040	-0.021
252800	-0.034	-0.045	-0.036
252810	-0.143	-0.072	-0.028
253112	-0.011	-0.003	-0.002
253420	-0.107	-0.117	-0.075
253430	-0.298	-0.159	-0.112
253440	-0.280	-0.105	-0.050
253450	-0.241	-0.165	-0.105
253460	-0.156	-0.146	-0.094
253470	-0.125	-0.107	-0.065
253561	-0.417	-0.317	-0.142
253562	-0.004	-0.002	0.000
254450	-0.011	0.000	0.000
254460	-0.014	0.000	0.000
254560	-0.018	0.000	0.000
254570	-0.017	0.000	0.000
254581	-0.009	0.000	0.000
254582	-0.014	-0.015	-0.013
254610	-0.025	-0.031	-0.034
254621	-0.062	-0.078	-0.087
256210	-0.012	-0.016	-0.010
256240	-0.013	-0.016	-0.013
256260	-0.013	-0.016	-0.013
256270	-0.013	-0.016	-0.012
256420	-0.013	-0.016	-0.013
256520	-0.010	-0.013	-0.014
256530	-0.010	-0.013	-0.014
256540	-0.010	-0.013	-0.014
256650	-0.010	-0.012	-0.014
256680	-0.010	-0.013	-0.014
256690	-0.010	-0.013	-0.014
256800	-0.013	-0.016	-0.013
256810	-0.013	-0.016	-0.013
256821	-0.028	-0.035	-0.039
256822	-0.010	-0.013	-0.014
256830	-0.006	-0.001	0.000
256880	-0.006	-0.001	0.000
256890	-0.007	-0.002	0.000
256910	-0.011	-0.003	-0.002
256920	-0.008	-0.004	-0.002
256932	-0.010	-0.003	-0.002
256942	-0.007	-0.002	-0.001
256970	-0.009	-0.002	-0.001
256982	-0.008	-0.003	-0.002
256990	-0.009	-0.003	0.000
257002	-0.011	-0.003	-0.001
257010	-0.023	-0.023	-0.022

257020	-0.006	-0.001	0.000
257050	-0.023	-0.022	-0.022
257060	-0.023	-0.023	-0.023
257072	-0.023	-0.023	-0.023
257080	-0.005	-0.001	0.000
257090	-0.005	0.000	-0.001
257110	-0.006	-0.001	0.000
257120	-0.007	-0.001	0.000
257130	-0.010	-0.003	-0.002
257140	-0.006	-0.001	-0.001
257150	-0.009	-0.002	-0.001
257160	-0.008	-0.003	0.000
257222	-0.010	-0.003	-0.001
257240	-0.007	-0.003	-0.001
257250	-0.007	-0.003	-0.001
257260	-0.010	-0.002	-0.001
257270	-0.023	-0.023	-0.023
257312	-0.009	-0.003	0.000
257322	-0.006	-0.002	0.000
257330	-0.007	-0.002	-0.001
257340	-0.017	-0.017	-0.017
257352	-0.006	-0.002	0.000
257360	-0.020	-0.019	-0.019
257392	-0.005	-0.001	0.000
257400	-0.006	-0.001	0.000
257410	-0.006	-0.001	0.000
257500	-0.010	-0.013	-0.014
269390	-0.011	-0.003	-0.001
270680	-0.005	-0.002	-0.001
829686	-0.259	-0.327	-0.366
832630	-0.172	-0.209	-0.232
